UNIVERSITY OF CALIFORNIA
RIVERSIDE

Self-Interference Cancellation in Full Duplex Radios and LTE-Unlicensed

A Thesis submitted in partial satisfaction
of the requirements for the degree of

Master of Science

in

Electrical Engineering

by

Chaitanya Umesh Mauskar

March 2016

Dissertation Committee:

Dr. Yingbo Hua, Chairperson
Dr. Ertem Tuncel
Dr. Jiasi Chen

The Dissertation of Chaitanya Umesh Mauskar is approved:

Committee Chairperson

University of California, Riverside

Acknowledgments

I am grateful to my advisor Dr. Yingbo Hua for his constant motivation and generous help for the thesis work. Without his guidance and advice this would never have been possible. Thanks to my parents for their love and support. Also I am thankful to my lab mates Qiping Zhu, Niraj Patel, Habib Gharavi, Yifan Li and Yiming Ma for providing me the help whenever I needed it and encouraged technical conversations.

ABSTRACT OF THE DISSERTATION

Self-Interference Cancellation in Full Duplex Radios and LTE-Unlicensed

by

Chaitanya Umesh Mauskar

Master of Science, Graduate Program in Electrical Engineering
University of California, Riverside, March 2016
Dr. Yingbo Hua, Chairperson

All the commercial radios are half duplex in a sense that they are unable to transmit and receive at the same time on the same frequency. A full duplex radio simultaneously transmits and receives at that same time and on the same frequency thus doubling the throughput of the existing systems. One of the fundamental challenges in enabling full duplex is the cancellation of the self-interference that is caused by device's own transmitter. Considering the high level of the self-interference at the receiver front end, it is necessary to cancel out the interference in the analog domain to avoid the ADC saturation. As one of the major focus of this thesis, all the existing methods, algorithms and accomplishments in enabling full duplex have been summarized. A novel method for interference cancellation using cables, power splitters and step attenuators has been implemented on the actual hardware and its performance evaluation and limitations have been summarized.

Currently deployed cellular networks use bands which have been licensed and approved by the FCC. With the developments in cellular standards Rel-10 LTE advanced which supports carrier aggregation has been established where a multiple carriers are aggregated to provide a larger bandwidth. As cellular operators explore the possibility

of extending the carrier aggregation to the unlicensed spectrum in the 5GHz, current developments in creating a friendly ecosystem in unlicensed bands have been summarized which form the basis of Rel-13 LTE- Licensed Assisted Access.

Contents

List of Figures

List of Tables

Part I

Self-Interference Cancellation in Full Duplex Radios

Chapter 1

Introduction

All the currently deployed wireless systems are half duplex. These radios establish the communication link by the use of different time slots (TDMA Figure 1.1) where sets of different time slots are assigned to the transmitter and the receiver to carry out their operation or different frequency bands (FDMA Figure 1.1) where transmitter and receiver function at completely different frequencies. As the valuable spectrum becomes more and more congested because of the exponential increase in the number of subscribers and devices it necessitates the use of more than the allocated bands and efficient use of the spectral resources. Although resourceful utilization is intricate but possible, the allocation of the bands is strictly regularized by the Federal Authorities thus rendering the development of the new technologies essential. One of such technology is full duplex which has received a significant consideration in both academia and the industry. Full duplex can improve the throughput of the cellular networks by mitigating the inter-cell interference and improve the throughput of the Wi-Fi networks by rendering the self-interference negligible.

Also Full Duplex can find applications in military to combat jamming from enemies and establish link with the friend. Full duplex radios unlike their half-duplex peers are capable of transmitting and receiving at the same time and in the same frequency band, Figure 1.1.

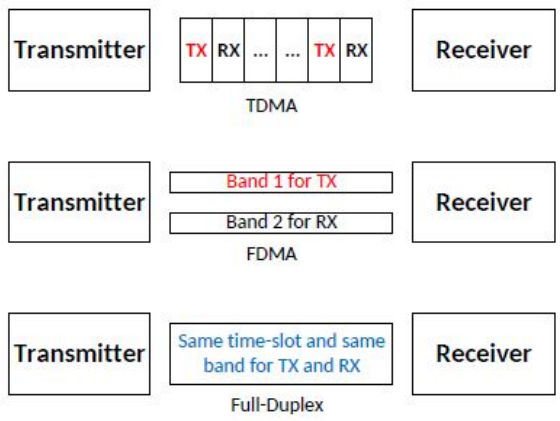

Figure 1.1: Radio Operating Modes

Thus full duplex radios have double or nearly double efficiency compared to half duplex radios. But there is a fundamental impediment in empowering the full duplex radios. When any device transmits it causes a strong interference to its own receiver (thus the name self-interference) which prevents it to listen on the same frequency as it masks the million times weaker desired signal (Figure 1.2). Thus to enable the simultaneous transmission and reception in the same band the cancellation of this self-interference (SI) is essential. While it may seem simple by attenuating the signal from transmitting antenna by increasing the antenna distance or by shielding (passive methods), there is a limit imposed on the maximum antenna separation due to the small size of the devices and thus still falling short of the enabling requirements of the full duplex by a big margin.

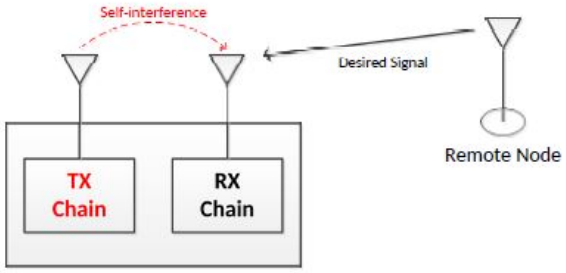

Figure 1.2: Self-Interference

Hence there is a need to develop a mechanism that will actively bring down the self-interference to the noise floor of the system so that a receiver can sense the weaker signal coming from the desired source and decode it correctly. The elimination of self-interference (SI) is never perfect and leaves some residual interference in the system after cancellation whose power is proportional to the power of the SI signal and thus increases the overall noise floor of the system and corrupting the desired signal.

Chapter 2

System Requirement and Early Development

2.1 Requirements

The standard 802.11 Wi-Fi signals are transmitted at a power of around 20dBm and with a noise floor of -90dBm there is a need to provide 110dB of total interference suppression to bring down the self-interference signal to the noise floor so that the desired signal can be received at the same frequency. Any amount of self-interference not cancelled will act as a residual self-interference and will increase the overall noise floor thus reducing the Signal to Noise Ratio (SNR).

As characterized by [1] the self-interference can be divided into 3 components.

1. Linear component: This component is contributed by the weighted copies of the known signal. It can be 110 dB above the noise floor.

2. Non Linear component: This is caused by the higher order harmonics terms introduced by the nonlinear components in the Transmit chain. It is about 80 dB above the noise floor.

3. Transmit noise: This is inherent in the transmit chain and is introduced by many components such as high power amplifier, phase noise of the oscillators and the IQ imbalance. It is about 60dB above the noise floor.

TYPES OF SELF-INTERFERENCE CANCELLATION

1. Passive cancellation: This is any passive mechanism of attenuating the SI before it reaches the receiver.

2. Analog cancellation: Cancelling the interference in the analog domain so as to prevent the ADC saturation and cancel out the strong interference. It can be done in the RF domain at the Rx frontend or in baseband before the ADC.

3. Digital cancellation: This aims to cancel out the residual interference left into the baseband in digital domain after the analog cancellation.

All these types (Figure 2.1) are discussed in more detail in the latter sections.

2.2 Early Developments

2.2.1 Full Duplex for narrowband AM and FM signals

Chen et. al [7] have shown a 72 dB of interference suppression method for 200KHz AM channel in division free duplexing. In this proposed dual antenna scheme total suppression consists of antenna path losses of 27dB, a RF echo canceller at the front end of the receiver to provide 37 dB of echo suppression. The digital filter is used

in the baseband to match the residual and to cancel it out. As shown in Figure 3 of [7] the AM carrier at 1.823 GHz and side tones have been suppressed well below the received FM signal.

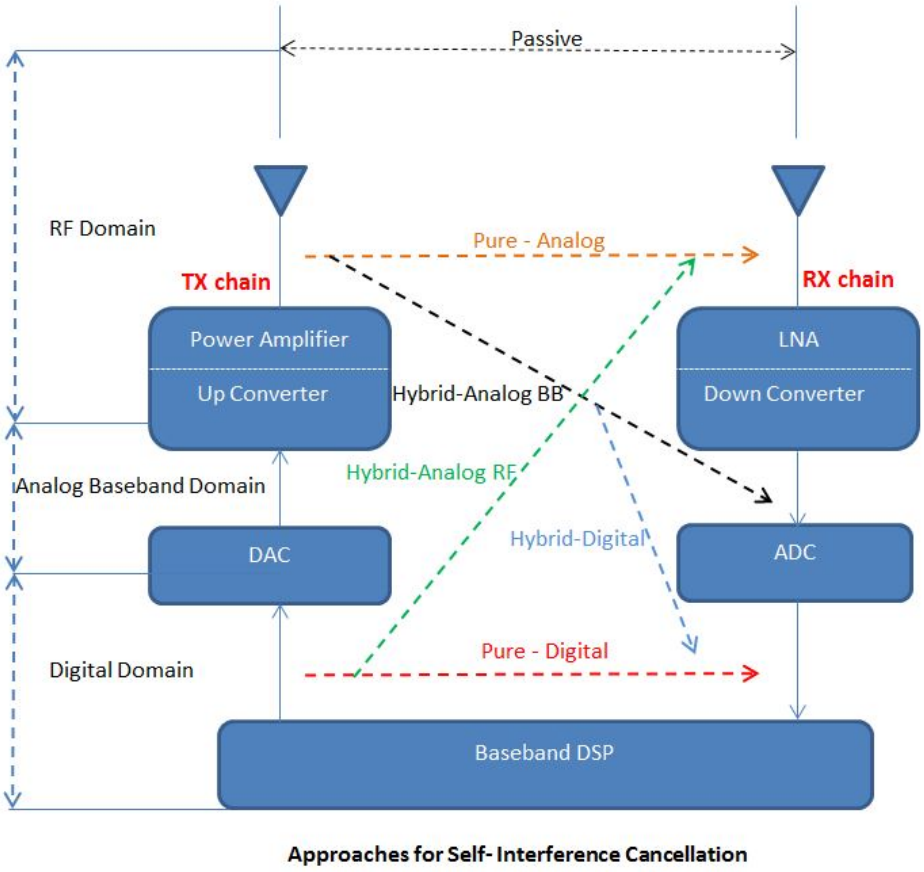

Figure 2.1: Types of Self-Interference Cancellation Mechanisms

2.2.2 Full Duplex for narrowband OFDM based DTB networks

The authors of [8] have proposed the cancellation method of the loop interference at the relay stations of the DTB (Digital Terrestrial Broadcasting) networks. DTB networks use 64 QAM modulated OFDM signals with 5.57MHz bandwidth. Pilot subcarriers are used in the OFDM scheme for the channel estimation and the detection purpose. These pilot signals have been used for the frequency domain estimation along

with the interpolation processing of the data subcarriers to obtain the transfer function of the FIR filter. Considering the disturbances in the loop interference channel, the estimation is done per every 2 OFDM symbols to update the filter coefficients. Simulations have reported the efficient cancellation of the interference given that ratio of the desired signal to the interference signal is less than 1dB. Figure3 in [8] shows the basic configuration of the proposed scheme.

2.2.3 Full duplex in the analog TV bands in comparison with ISM hosted Wi-Fi networks

Authors of [9] have argued that the use of lower carrier frequencies is more beneficial in indoor environments as the signal penetration is more at lower frequencies and this will yield a significant improvement and better connectivity. Also lower frequencies (within 470- 806 MHz in analog TV bands) exhibit more uniform propagation and need 100 times lower transmit power(or 1mW) than the existing ISM based WI-FI networks. This will simplify the network design and the deployment complexities. As mentioned in [9] the 30dB of cancellation of the unwanted self-interference signal is obtained in the analog domain using active component for echo cancellation QHx220 chip which subtracts the self-interference signal and thus enabling the decoding of the useful signal. The chip allows the changes in the phase and amplitude of the references interference input signal to match the interference at the receiver. An RF splitter has been used to pass a copy of the transmitted signal of a 20 MHz as an input to QHx220. Also a case of transmit antenna nulling using the directional properties of the antennas has been proposed to achieve a 25dB of more cancellation. A nulling antenna will form a null in the direction of its receiver thus preventing the SI to leak while radiating the main beam in the desired direction.

Chapter 3

Passive Cancellation and Antenna Cancellation

3.1 Passive Cancellation

The transmit signal from the Tx antenna is attenuated over the air because of path losses before it reaches the Rx antenna. In case of using a single antenna with the isolator, the isolator provides some isolation (around 15 20dB) between the Tx and the Rx chains. So with the case of a single antenna, transmit power of 20dBm and after the isolation of around 30 dB the self-interference will be -10dBm at the receiver front end, still being stronger than the weak -70dBm desired signal and nonetheless preventing the full duplex operation. This approach of increasing the path loss by increasing the antenna distance (or isolation by the circulator in single antenna case) or introduction of any shielding or absorbing material is termed as the passive self-interference cancellation.

Following table lists the various approaches proposed for passive mechanism of self-interference cancellation. Everett et. al in [10] have presented the capabilities, effects and limitations of the passive cancellation. The characterization is based on 3 passive suppression mechanisms.

Table 3.1: Passive Cancellation Mechanisms

Antenna Placement & Destructive Addition	[11],[12],[13],[14],[15]
Cross Polarization	[16],[17],[18],[19],[20]
Directionality & Beamforming	[21],[10],[16],[17],[20],[22],[23],[24],[25]
Antenna Separation & Absorptive Shielding	[20]

1. Cross polarization: Use of orthogonal polarization for transmission and reception.
2. Directivity of antennas: Use of directive antennas such that Tx and Rx have the low gains in each other's direction.
3. Absorptive materials: Use of absorptive materials to increase the path losses.

The effect of directivity for suppression has been evaluated with 5 different antenna configurations as seen from the Figure1 in [10]. Different beam widths with different antenna spacing have been used for the measurement. This topic of antenna directivity has been analyzed more in detail in [21] by placing mobile station with respect to the base station at different angles and also in [20] supporting 4096 reconfigurable antenna radiation patterns. Placement of the antennae inside the devices also plays a significant role in passive cancellation. Different placement tactics have been explored in [13]. Figure3 in [13] and Table I in [13] present the experimental results. Placing 3 Tx antennas on the vertices of the equilateral triangle and the Rx antenna at the centroid along with the analog cancellation forms the basis of the FlexRadio design presented in

[14].The cancellation signals from the 3 Tx antennas are phase shifted by π and combined at the Rx antenna to cancel out the SI.

Absorptive shielding has been evaluated with the use of Eccosorb AN-9 absorber in [10]. L-com HGV-2406 antennas supporting vertical and horizontal polarization have been used to evaluate the suppression by cross polarization. Table I in [10] summarizes the effects of different parameters on the achieved passive suppression. Whenever the signal travels in the environment there are always multi path reflections resulting from the objects in the vicinity. Hence apart from the main direct signal component from Tx to Rx there any many reflected replicas of the signal reaching the Rx antenna. The impact of environmental reflections on the performance has been summarized in [10]. These environmental reflections become the bottleneck in suppression even though the mechanism is effectively suppressing the main direct path signal (Line of Sight signal), it is ineffective against the reflected copies of the self-interference (Non line of sight components). This implies that the existing infrastructure should have the least number of objects (reflectors) in its neighborhood, which is intolerable because of the practical concerns. The argument in [10] that the passive cancellation decreases the coherent bandwidth and leads to frequency selectivity gives rise to a question that: if there is any relation between the active cancellation and the passive cancellation and in what case the combination can achieve the best result.

3.2 Antenna Cancellation

3.2.1 Antenna reflection coefficient matching

As proposed in [26] the isolation in Tx and Rx chains is proportional to the reflection coefficient S_{11} or ζ_{Ant} of the antenna. In this approach with the use of a single

antenna and isolator the electrical balance duplexing has been employed. Impedance mismatch of the antenna leads the SI to leak into the Rx chain. The EB (electrical balancing) duplexer matches the reflection coefficient of the antenna ($\zeta_{Bal} = \zeta_{Ant}$, where ζ_{Bal} and ζ_{Ant} are the complex reflection coefficients of the Electrical balancing network and the antenna respectively) and tries to cancel the reflections. Figure1 in [26] gives the diagrammatical representation of the EB network. Although simple to achieve, the balancing at the carrier frequency yields poor isolation at other frequencies in the transmission band. The optimal balancing can be achieved with MMSE algorithm and the use of frequency flat first order RC or RL networks as given by the following equation(4) in [26] .

$$G_{Tx-Rx_{MMSE}} = min_{\zeta_{Bal}\{\overline{L|\zeta_{Bal}=\zeta_{Ant}(w)|^2}\}} \tag{3.1}$$

for $w_l < w < w_h$, where w_l, w_h are lower and upper bounds respectively.

A slight offset in the coefficients and reflections from the environment need to be taken into the consideration which affect the performance significantly. The results have shown 60dB isolation for 20 MHz bandwidth but the isolation worsens as the bandwidth widens. The similar approach has been proposed in [27] with the use of quad hybrid and balancing network over a band of 860MHz - 960 MHz. While [18] and [19] have proposed the EB duplexing approach for SIC in the 2.4GHz ISM band.

3.2.2 Asymmetric antenna placement for destructive superposition

While nearing the realm of existing WI FI networks Choi et. al [11] have proposed the antenna cancellation method for 5MHz 802.15.4 (ZigBee) standard combined with digital cancellation. The main idea proposed is to use 2 transmit and one receive antennas where the 2 transmit antennas are placed at a distance of d and $d + \frac{\lambda}{2}$ from the receive antenna, Figure2 in [11]. Keeping the offset of $\frac{\lambda}{2}$ causes the signals from

transmit antennas to have a phase difference of π and thus to add destructively at the receiver and cancel each other. Destructive interference is most effective when the signal amplitudes at the receiver from both the antennas match.

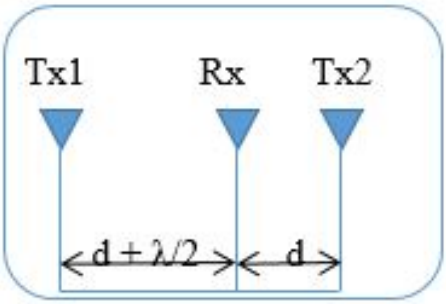

Figure 3.1: Asymmetric Antennae Placement

However with unequal receive power from both the antennas still there is some non-zero signal power even if the signals combine perfectly out of phase. With this method it is possible to achieve the 30dB reduction in the SI signal and combining with the analog cancellation method in [9] and digital cancellation technique around 60dB cancellation can be achieved for the case of 802.15.4 systems with a transmit power of 0dBm and -40dbm SI power at the receiver and -100dBm noise floor. But the performance of this design is severely impacted as the bandwidth of the signal increases. This can be attributed to the narrow band QHx220 echo canceller and thus yielding poor performance in the wideband 802.11 WI FI systems.

3.2.3 Symmetric antenna placement for destructive superposition

The similar concept [12] of the phase difference of π can be used in cancelling the SI signal with equidistant placing of the Tx antennas from the receive antenna.

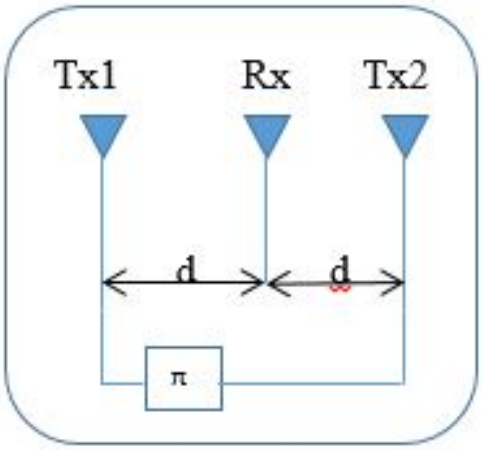

Figure 3.2: Symmetric Antennae Placement

In this case one of the Tx antenna is fed with signal shifted by π using phase shifter, while another Tx antenna is fed with the 0 degree phase shifted (original) signal. The same symmetric placement can be applied in case of 2 Rx antennas and one 1 Tx antenna. This eliminates the bandwidth constraint as imposed in [11] by the antennas since the phase shifters have better frequency response and also the need of perfect asymmetric placement of antennas by d and $d + \frac{\lambda}{2}$ is eliminated. But the offset and the insertion loss of phase shifters plays a noteworthy role.

Similar as the approach of antenna cancellation in [11] and [12] a balanced symmetric design based on 2 antennas and 2 circulators has been proposed in [15]. The receiver experiences 3 types of interferences namely SI leakage, reflections due to the antenna impedance mismatch and the cross talk. A combiner is used at Rx front end to combine the Port3 of both the circulators. Being symmetric if antennas and circulators

are properly matched the structure attempts the SIC and also tries to cancel the cross talk. The main intuition of this approach to use the symmetric circuit to generate the SI with the opposite phase. Figure1 in [15] represents the proposed structure. Any discrepancies in circulators degrade the cancellation performance.

Chapter 4

Analog and Digital Cancellation

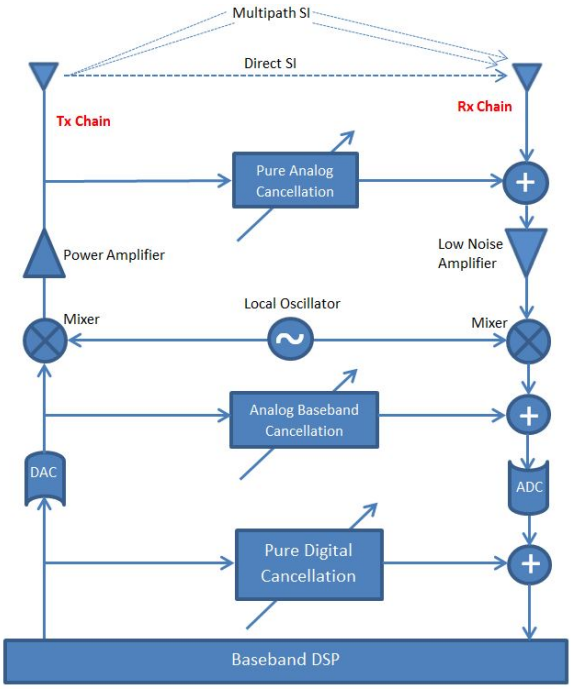

Figure 4.1: Analog and digital cancellation approaches

4.1 Analog Cancellation

4.1.1 Balun based Picasso Design

Authors Hong et.al have proposed the method of spectrum slicing in [28] where a spectrum can be partitioned into different arbitrary slices with each fragment running a different protocol such as OFDM PHY and CSMA MAC. Such ability can also be used for simultaneous transmission and reception and developing co-existence strategies in small size devices where the area available on the board to place the components is of paramount importance. The main contribution of the Picasso design in [28] is to partition the available spectrum into multiple slices with a single antenna, one Tx and Rx chain and to provide the abstraction of a single narrowband radio on each allocated spectrum slice to the higher level protocols. The slicing of the radio font end and use of a Balun (balanced unbalanced transformer) for signal subtraction and active QHx220 yields cancellation of around 35dB for 40 MHz signal but is insignificant for the operation of Picasso as sufficient isolation between adjacent bands can't be provided. The QHx220 leaks a lot of self-interference in the adjacent spectrum and thus reducing the SNR and affecting the performance severely. Also QHx220 introduces many complications such as non-linearities and distortions. Hence to avoid the leakage it is desirable to use the passive, leakage free components. This can be achieved simply with the use of fixed phase shifters and programmable attenuators.

The use of delay lines and programmable attenuators makes it possible to account for the phase offset and range of other perturbations and thus to mimic the RF interference. The programmable filtering engine has been used in this approach in the baseband for resampling, filtering and mapping to the appropriate spectrum slices.

This idea of using programmable attenuators and shifting phase forms the foundation of the many other analog cancellation techniques. [5, 51, 59]. While it may seem simple to obtain a copy of the transmit signal in the baseband and subtract it from the SI signal at the receiver, it is not enough and accurate and leaves a lot of residual interference in the system. The reason being although the radio knows what it is transmitting in the baseband; many other modifications are added to the signal when it is converted to the analog domain by the DAC (Digital to Analog converter), translated to the carrier frequency by the LO (Local Oscillator) and the mixer; and high power amplifier (PA) which is used to raise the power of this up-converted signal. All these analog components introduce individual noise and non-linearities to this signal which are unknown to the radio in the baseband. Hence being unable to model these distortions in the baseband, thus it is necessary to subtract the signal at the receiver front end in the analog domain.

There are two contemporary methods to cancel the signal in the analog domain.

1. Use of an auxiliary transmits chain to create an antidote signal and subtract the SI at the receiver.

2. Use of a signal inverter and/or phase shifters and variable attenuators to match the SI at the receiver.

4.1.2 Use of Auxiliary Transmit Chain

The figure1 in [29] represents the architecture in the 1^{st} approach proposed by Duarte et.al in [29]. Here the signal before being converted to the analog by the DAC is fed into the auxiliary transmit chain and is after up converting and attenuating, combined with the SI signal from the primary transmit antenna. The cancellation signal

in the auxiliary transmit chain is generated in a fashion such that it is opposite of the SI signal and thus attempts to cancel out the SI signal. Following equation gives the mathematical description of the approach

$$Y(f) = (h_I(f) - h_z(f)\widehat{K_{AC}}x(f) + h_D(f)z(f) + w(f) \tag{4.1}$$

Where $h_I(f)$ is the SI channel, $h_z(f)$ is magnitude and phase changes affecting the cancellation signal and $\widehat{K_{AC}}$ is the noisy imperfect estimate of K_{AC}. While $h_D(f)$ is the channel between the desired source and the receiver and $z(f)$ is the desired signal and $w(f)$ represents the noise. The cancellation is perfect if

$$\widehat{K_{AC}} = K_{AC}$$

such that

$$h_I(f)x(f)_{RF} - h_z(f)\widehat{K_{AC}}x(f)_{RF} = 0 \tag{4.2}$$

Authors in [30] have suggested the use of steepest descent for the channel estimation. Performance of LMS and RLS are similar for the narrowband signals however the performance of the LMS worsens for the wideband signals in overall yielding 30 dB of cancellation while the fast converging, purely algebraic RLS algorithm is robust to the wideband signals.

Similar to the approach in [29] of using the auxiliary transmit chain for SIC, Askar et. al [31] have proposed the method DPD(Digital Pre-Oder Distortion). In this approach the training based pilot signals are used for parameter acquisition phase where the channel is estimated. Based on the acquired parameters, distortions in the channel are modelled. Two models namely linear and non-linear distortion models have been developed. Equations (6) and (7) in [31] give the mathematical description of linear and

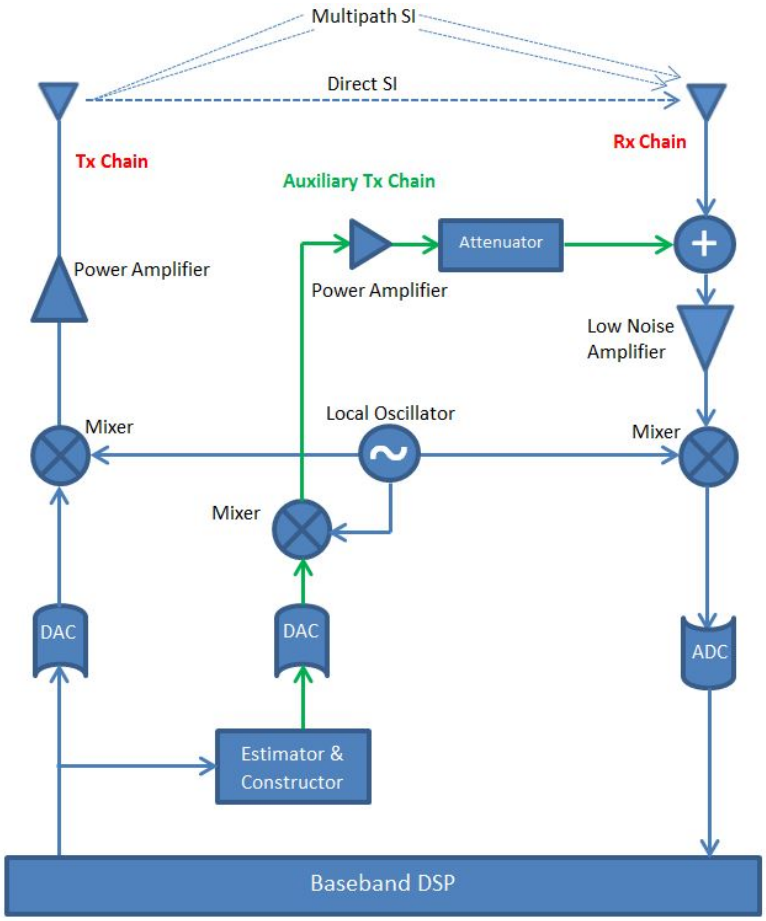

Figure 4.2: Use of auxiliary chain for cancellation

non-linear models respectively. Non-linear model closely models the non-linearities in the transmit chain and performs better than the linear model however the construction time for non-linear model is more than that of the linear model. This modelled distortion is then constructed in the baseband and applied in the inverse way (negative amplitude) and then fed to the auxiliary transmit chain so as to perfectly cancel the SI. The experimental data reports 28dB of cancellation by linear DPD model and 30dB by non-linear model. The limited amount of cancellation is attributed to the factors such as phase noise and the IQ imbalance which have been considered in other works.

4.1.3 Balun based signal inversion

Eradicating the bandwidth constraint imposed by the antenna cancellation methods (inversion by π with d and $d + \frac{\lambda}{2}$), where antennas give perfect inversion at carrier frequencies but perform poorly with imperfect antenna spacing and when signal moves away from the carrier frequency; Jain et.al in [32] have explored the 2^{nd} approach. In this a Balun is used to acquire the inverted copy of the SI and is fed through the attenuators and the delays (QHx220) to perfectly match the RF interference. This inverted signal is combined with the SI at the receiver to cancel the SI. This technique demonstrated the 40dB cancellation for a wideband 100MHz signal. Figure3 and Figure7 in [32] represent the block diagram of the proposed system. This however has some limitations introduced due to the nonlinear behavior of the QHx 220 and non-frequency flat Balun which not always yields the perfect inversion. The structure also requires the precisely programmable delays.

4.1.4 Phase change with delay lines of Sinc Interpolation approach

Bhardia et.al in [1] have offered the Sinc interpolation approach. In this a small RF reference is obtained from the transmitter after the PA and is fed to the cancellation circuit consisting of variable delays and variable attenuators. The fixed lines consisting of delays and attenuators are summed up for signal reconstruction and later combined with the SI signal at the RF front end. Delays are used to obtain the leading and lagging copies of the transmit signal and programmable attenuators are used to adjust the amplitude of these copies. Thus the tapped signal can be represented as the weighted linear combination of the SI signal and consequently configuring these parameters serves to match the SI and cancel it. This approach mainly benefits from the use of leakage

free passive components. Experimental data here reports 45dB of analog cancellation with 8 delay lines. While impressive this structure needs uniform time delays and the performance is severely impacted by the choice of the carrier frequency as shown in [33].

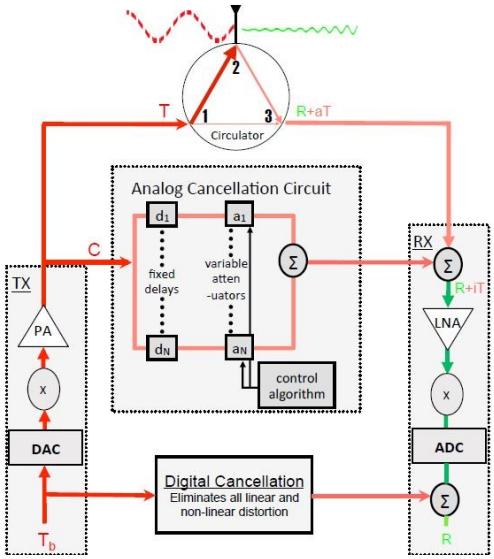

Figure 4.3: Analog cancellation with delay lines [1]

4.1.5 Phase change with power splitters

Being based on the concept of phase shift and attenuation Authors in [33] have proposed a clustered architecture of the analog canceller eliminating the need of precise delay lines, where each clustered tap consists of 4 programmable attenuators and 3 power splitters. Each power splitter splits the input signal into two differing copies from each other by the phase of 90 degrees. Thus 4 copies of the tapped reference are fed to programmable attenuators with a successive phase shift of 90 degrees thus covering the complete 360 degree complex attenuation plane and are later combined with the use of a power combiner and used at the Rx front end for the analog cancellation. A

novel method in the later part of this dissertation mainly focuses on the mathematical formulation and experimental evaluation of this approach.

This approach does not need precise delay lines as used in the uniform architecture in [1] and is robust to the carrier frequency. The similar approach of shifting the phase by 90 degrees by the use of 4 delay lines $0, \delta, 2\delta$ and 3δ(such that each delay $\delta = 1/4$) has been shown in [34]. Simulation results in [33] have shown 77 dB of overall analog cancellation with the use of 2 stage canceller consisting of 1 clustered tap in the first stage and 3 clustered taps in the 2^{nd} stage.

4.1.6 Use of variable phase shifters

Instead of using power splitters to obtain the phase shifted versions of the incoming signals McMichael et. al have proposed the use of variable phase shifters in [2]. As the non-convexity of the standard optimization returns many local optima and thus yielding poor cancellation, this approach formulates the optimization problem of the tuning of the canceller as the convex giving a global minima. The proposed method tries to minimize the mean squared error and thus obtaining the optimal weights which are applied in an inverse way thus to cancel the RF interference. Simulations have shown 65dB of cancellation from the proposed method combined with the antenna cancellation.

4.1.7 Phase rotation at the subcarriers

The delay experienced by the interference channel rotates the phase of the baseband signal at each subcarrier. Authors of [35] have leveraged this fact and have suggested the use of Maximum Likelihood estimation algorithm in which the algorithm estimates the phase rotation and gain experienced by the baseband signal at each sub-

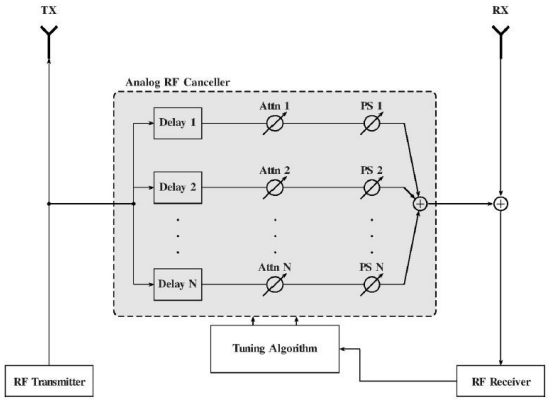

Figure 4.4: Analog Canceller with variable phase shifters [2]

carrier after demodulating the SI in the training period. This estimation is used to rotate the phase of the baseband signal at each subcarrier in a way such that it will match the RF interference. The phase rotation can be implemented with a baseband operation without the use of programmable attenuators and phase shifters. After applying the phase rotation the signal is amplified with the estimated gain and this data is fed to the auxiliary transmit chain where it is mapped onto the subcarriers and up-converted and amplified.

Figure 1 in [35] represents the proposed approach. This antidote signal is then combined in front of the receiver to cancel the SI. While comparing the performance against the method in [32] where the cancellation degrades for the subcarriers away from the carrier frequency, this method provides uniform SI cancellation for all the subcarriers in the transmit signal.

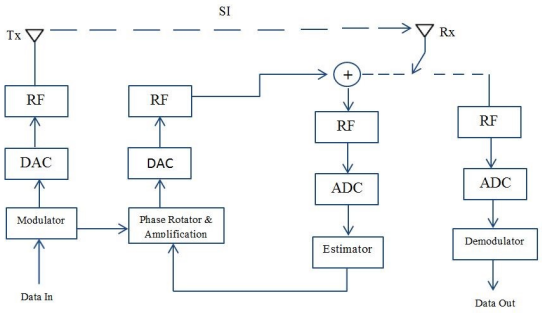

Figure 4.5: Phase rotation at baseband subcarriers

4.1.8 Analog Baseband cancellation approach

Even though it is possible to cancel the 40-45 dB of interference in the RF stage there is still a need to cancel the 40dB of interference out of which 30 dB is caused because of the transmission noise induced in the transmit chain. The approach of using the auxiliary transmit chain to generate the cancellation signal suffers if the desired signal is 50dB lower than the interference signal. All the above methods attempt to cancel the SI before the Low Noise Amplifier (LNA) of the receiver.

The Hybrid-2 approach has been proposed in [36] where the self-interference in analog is down converted and digitally filtered yielding analog baseband cancellation signal which is combined with the analog baseband SI before the ADC of the receiver. This approach models the interference channel in the Tx and Rx antennas (or the leakage path of the isolator) and the channel between the Rx antenna and the analog baseband combiner before the VGA. Depending on the choice of the training vectors the optimal response of the digital filter can be computed in the absence of the desired signal by the proposed method so as to cancel the SI in the baseband. The experimental data reported shows a 50dB SIC for 15 MHz wide signal. Authors Kaufman et. Al in [37] have proposed a similar argument that conventional RF stage analog cancellation can be

complemented with the baseband analog cancellation to augment the performance. In this approach the baseband signal after the DAC is tapped and combined in a fashion just before the ADC of the receiver such that it tries to cancel the interference in the baseband. Figure 2 in [37] shows the analog baseband SIC approach. In the absence of the desired remote signal the self-interference channel is estimated using recursive least square algorithm and obtained weights are applied on the tapped baseband signal as to mimic the baseband SI signal. The simulations demonstrate the 10dB increase in the signal to interference and noise ratio (SINR) for signal centered at the carrier frequency of 2.435GHz.

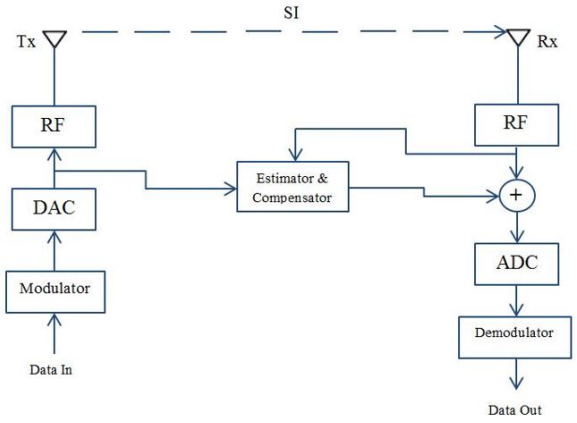

Figure 4.6: Analog baceband cancellation approach

4.2 Digital Cancellation

4.2.1 DSIC with noisy channel estimation

The main goal of the digital cancellation is to clean out the residual left after the analog cancellation. In digital cancellation a copy of the baseband digital signal is passed as a reference such that it attempts cancel out the residual SI after the ADC in the receiver. As proposed in [29]

$$(h_I(f) - h_z(f)\widehat{K_{AC}})x_{RF}$$

is the residual after analog cancellation. Digital cancellation is applied on a frame by frame basis such that

$$\widehat{K_{DC}} = h_I(f) - h_z(f)\widehat{K_{AC}}$$

during nth frame and hence the interference cancelled after analog and digital methods is represented by

$$Y(f) = (h_I(f) - h_z(f)\widehat{K_{AC}} - \widehat{K_{DC}})x(f) + h_D(f)z(f) + w(f) \tag{4.3}$$

Where $\widehat{K_{DC}}$ is the noisy estimate of K_{DC}.

The interference channel for each subcarrier in an OFDM packet can be estimated with the use of RLS algorithm in the frequency domain. Known training symbols at the beginning of the OFDM packet are used for the channel estimation. The FIR filter can be used to mimic the time domain response of the estimated channel such that after the linear convolution of the reference baseband samples and the response of the FIR filter, digital samples are generated to cancel out the interference in the digital domain. This method has been proposed in [32]. However the non-linearities and other sources affect the channel estimation process thus yielding the imperfect noisy estimate. Also the low coherence time of the channel makes re-estimation and retuning necessary. This

method has shown 25-30 dB of digital cancellation for 10 MHz OFDM signal. While being based on the same concept of sending the known training symbols (2 symbols in the OFDM preamble) the response of the channel can be calculated as

$$y = Ah + w \tag{4.4}$$

Where A is known matrix as shown by 3.2.1 in [1] and thus it can be precomputed to obtain the MLE (maximum likelihood estimate) of the interference channel. The column wise pseudo inverse of $A(a_i^+)$ is obtained to model the linear distortions in the interference channel. The higher order non-linearities reflected in the baseband are computed using 3.3.2 in [1] which attempts to provide 20dB of non-linear digital cancellation.

4.2.2 DISC with Auxiliary receive chain

Unlike previous approaches where a baseband signal is passed for the digital cancellation, a relatively different approach can be employed with the auxiliary receive chain [38]. The auxiliary receive chain consists of all the same elements as that of the primary receive chain such as down converter (mixer), ADC and FFT (for un-mapping the data from the subcarriers in the OFDM framework). The LNA is not needed in the auxiliary receive chain since the reference can be directly obtained after the power amplifier with the use of a coupler or a wired attenuated connection. The difference between the data received in the auxiliary and the primary chain is used to estimate the interference channel based on the training symbols in the OFDM preamble. This estimated channel is later multiplied with the digital samples in such a way that its subtraction from the data in the primary receiver chain removes the SI in the digital baseband. However channel estimation accuracy is dependent on factors such as Gaussian noise, quantization noise, non-linearities, number of training symbols used and coherence time

of the channel. This attempts to mitigate the transmitter and receiver non-linearities (PA at Tx and LNA at Rx) and the quantization noise caused by the ADC. Phase noise of the receiver is mitigated by sharing the PLL between the auxiliary and the primary receiver chain. The comparison of this approach with the conventional digital cancellation approach is tabulated in Table I of [38]. This approach can be combined with the analog cancellation approach [39] such that the tapped RF reference is used for analog cancellation at the RF front end while the down converted digital reference is used for the digital cancellation.

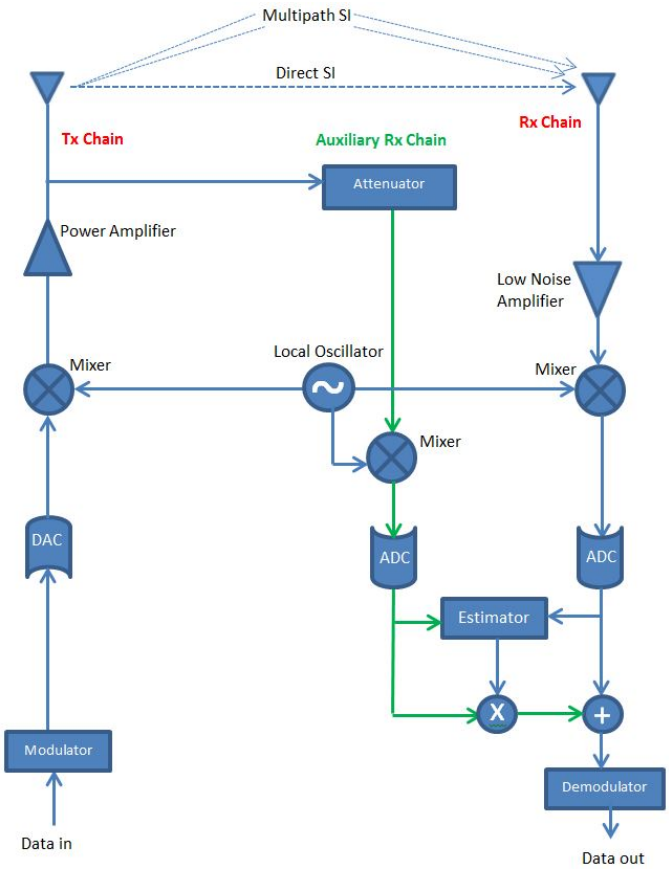

Figure 4.7: Auxiliary receive chain for cancellation

4.2.3 Compensation for channel estimation errors due to the presence of the desired signal

The channel estimation in SIC is never perfect because the desired signal coming from the remote node acts as a noise in the estimation process of the self-interference channel and worsens the estimation. A two stage iterative channel estimation and algorithm is proposed in [40].The signal after the PA in the transmit chain is coupled and down converted and fed to the ADC to obtain the reference in the digital domain for the cancellation. The coupled signal is sampled at the frequency multiple of the Baud rate to obtain the precision in cancellation. Figure 2 in [40] represents the block diagram of this approach. First in the presence of the desired signal a rough estimate of the SI channel is obtained and rough cancellation is applied which compensates for the IQ imbalance and the frequency offset in the transmit chain. In the second stage while demodulating the desired signal, IQ imbalance and frequency offset in the desired signal are estimated. The received OFDM data is re-modulated at the Rx end and constructed with the IQ imbalance and frequency offset of the desired source. These constructed parameters then compensate for the channel estimation of the SI which is corrupted by the presence of the desired signal thus yielding more accurate channel estimation of the SI and subsequently giving better cancellation. Simulation data reported here has shown 65dB of overall cancellation for 802.11 Wi-Fi signals. The simulation results in the similar approach by [41] report the 60dB of cancellation.

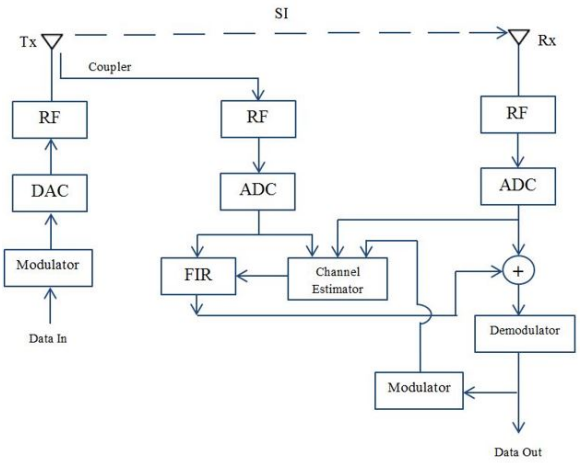

Figure 4.8: Iterative channel estimation in the presence of signal interest

4.2.4 Time domain transmit beamforming

A frequency domain transmit beamforming [1,3,9,41,42,45,49] method which yields frequency domain solutions needs frequency flat channels and is generally suited for the narrowband applications. This method thus is not sufficient to remove the SI in the time domain in the prefix region of the OFDM structure. To mitigate this, a time domain transmit beamforming can be employed with the use of auxiliary transmit chain at the RF frontend. The cancellation signal from the auxiliary chain can be coupled wirelessly (over the air) or can be connected directly via RF power combiner. In a general case this calculates the FIR spatial precoding weights spanning the null space of the MIMO channel matrix. The power of the SI in the prefix region can be represented by equation7 in [36] such that

$$P_I = P_X \sum_{l=n+1}^{L} |h_2(l)|^2; n = 0, 1, ..., L-1 \tag{4.5}$$

Where h_2 denotes the baud rate interference channel between primary transmit chain and the receiver. h_1 is the baud rate cancellation channel between the auxiliary chain and the receiver, L is the cyclic prefix length. After receiving the interference

samples, the auxiliary receiver transmits first L samples as

$$y_2[n] = -\sum_{l=0}^{L} h_2[l] v_{(N-L+n-l)_N} \tag{4.6}$$

So that the left SI in the prefix region is

$$y[n] = y_1[n] + y_2[n] = -\sum_{l=n+1}^{L} h_2[l] v_{(N-L+n-l)_N} \tag{4.7}$$

The experimental data here reports a 50 dB decrease in the INR (Interference to noise ratio) after the application of the proposed scheme. The channel estimation approach of the above TDTB method can be augmented by the iterative scheme in [42]. In the first phase the MIMO channel is estimated by the normalized LMS algorithm and in the next space basis spanning the null space of the SI channel is computed later to remove the null beam in the direction of the incoming desired signal by the choice arbitrary weights. The simulation results have shown a 40dB of interference cancellation by this scheme.

4.3 Combination of Active & Passive Cancellation Schemes

As characterized by [29] digital cancellation as a function of analog cancellation, DC is most effective if the suppression obtained in the analog stage is less and vice versa. Also it has been argued that if the power of the SI is more it yields better cancellation. This can be ascribed to the fact the strong SI assists in better channel estimation and thus assisting in more cancellation. This answers the question in which case the combination of passive and active cancellation mechanisms give the best performance.

Chapter 5

MIMO FD and FD Relays

5.1 Full Duplex MIMO Radios

The radios with Multiple Input Multiple Output (MIMO) antennas support the spatial multiplexing and improve the diversity. This is beneficial to support the parallel data streams transmission and capacity enhancement. However in MIMO the radios not only have to cancel the self-interference but also the cross interference (cross talk) originating from the other transmitting antennae which are relatively weaker than the SI. The structure of the SISO Full duplex designs can be replicated for the MIMO but it suffers from the complexity as the complexity in implementation for M antennae isM^2. Also for the MIMO, the residual interference is proportional to the number of antennas. Also it's necessary to keep the channel estimation errors below the accepted level to keep the noise low and avoid the dilapidation of the SNR.

A simple approach based on the symmetric placement of 2 Tx and 2 Rx antennas has been shown in [43] to provide the antenna cancellation. The data reported shows a 45 dB cancellation for a 650 KHz single subcarrier OFDM system at 2.484GHz. 37 dB cancellation at 2.474GHz shows an overall 35 dB cancellation over 20MHz band while

the performance drops below 20dB for 2.464GHz for 40MHz signal. This is attributed to the operation of the phase shifters providing precision for small frequency bands used in the symmetric placement. This approach suffers badly in the highly reflective environment. Placing the path antennas in symmetric manner and using orthogonal polarization simulations in [17] have shown a suppression of 21 dB in the transmitting antennas and 50dB in the receiving antennas for a 2 X 2 MIMO system.

With the use of National Instruments FlexRadio 5791R module supporting 2 X 2 MIMO configuration authors of [44] have experimentally showed a RF cancellation of 53dB for a transmit power of 4 dBm for a 20MHz signal based on the architecture proposed in [29]. Based on the SISO design in [45] authors of [46] have suggested its 2 X 2 MIMO extension. The design at the analog cancellation stage of each receive chain takes the reference to cancel to the self-interference and the cross talk. While the digital cancellation stage takes the reference from the digital baseband for the least square estimation of the interference channel. The simulation data with a 40dB antenna separation and 30dB of analog cancellation reports the SINR of 15dB with the developed cancellation model. Similar to [46] for a 2 X 2 MIMO instead of taking the reference for digital cancellation from the transmitter chain, reference receive chains have been proposed Figure 1 [47] to obtain the reference for digital cancellation. This reference receiver aided digital cancellation allows to account for the distortion induced in the transmit chain. The simulations have shown to obtain higher SINRs with the proposed scheme than the linear and non-linear digital cancellation schemes.

As opposed to the SISO replication the empirically evaluated cascaded design in Figure 4 [48] provides 18 dB better cancellation for a 3 X 3 MIMO. Also the less number of taps in the analog cancellation stage reduces the power requirement and suffices to reduce the tuning time for the taps. Also for the 2 X 2 MIMO the training method in

[48] makes use of 2 time slots for the digital cancellation which reduces the residual in the system. Instead of sending separate training symbols in different time slots, the technique here sends separate training symbols in the same slots thus sending 4 symbols in 2 time slots. This joint training method halves the residual interference power compared to the SISO case. The experimental data reports 25dB improvement compared to the SISO case for which the noise floor increases with the additional antennas.

5.2 Full Duplex MIMO Relays

Relays are used to expand the network coverage and quality enrichment with the facilitation of MIMO streams. Relaying is a multi-hop technique in which the relay node receives the data from the source and forwards it to the destination node which without relaying is out of the coverage of the source. There are 2 ways in which a relay serves its purpose.

1. Amplitude and Forward Relay (AFR)

   Simply amplify the incoming signal and forward it.

   Less complex and easily deployable

2. Decode and Forward Relay (DFR)

   Decode the incoming signal, clean out the noise, regenerate the message and forward.

   Relatively more complex but better performance.

When relay is transmitting a data received from the source to destination, its transmitter causes interference to its receiver listening to the source. This interference in relays is known as the loopback interference (LI) or the SI of the relay, Figure 5.1. To operate the relay in the full duplex mode, LI needs to be cancelled.

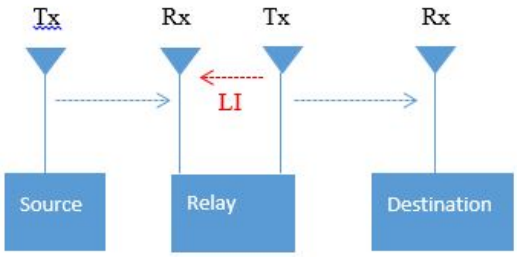

Figure 5.1: Relay System

The received signal at the relay can be written as

$$r(n) = H_{s-r}X_{s-r}(n) + H_{r-r}X_{r-r}(n) + n_r(n) \tag{5.1}$$

While the signal at the receiver of the destination can be represented as

$$y(n) = H_{r-d}x_{r-d}(n) + n_d(n) \tag{5.2}$$

where H_{s-r} is the channel between the source and the relay receiver, $x_{s-r}(n)$ is the data transmitted from the source, H_{r-r} is the loop interference channel between the relay transmitter and the relay receiver, H_{r-d} is the channel between the relay transmitter and the destination receiver, $x_{r-r}(n) = x_{r-d}(n)$ is the data transmitted from the relay, $n_r(n)$ is the additive white Gaussian noise (AWGN) at the relay receiver and $n_d(n)$ is the AWGN at the destination receiver.

Also $x_{r-r}(n)$ can be expressed as

$$x_{r-r}(n) = W_t G W_r r(n) \tag{5.3}$$

W_t is the transmit weight cancellation matrix and W_r is the receive weight cancellation matrix applied by the relay for LI suppression. Since the relay knows what it is transmitting, relay can subtract this transmitted signal from the data received at its input for the LI cancellation if the LI channel is known. This can be done with the combination of analog and digital cancellation. This method is known as the Time domain cancellation [TDC] but is not purely perfect as there are errors in the estimation of the CSI matrix and an unknown noise is added to the LI.

The SVD of the LI channel H_{r-r} can be written as

$$H_{r-r} = U \sum V^H \tag{5.4}$$

where U and V are unitary matrices containing the left and right singular vectors respectively while $\sum$ is the diagonal matrix with non-negative diagonal elements known as the singular values. The rank of this H_{r-r} has the minimal effect on TDC but the performance of NSP highly depends on the rank of H_{r-r}.

W_t&W_r are chosen in a way such that

$W_t \in$ Right null space (H_{r-r})

$W_r \in$ Left null space (H_{r-r})

This orthogonal subspace projection causes the suppression of the self-interference. This approach is known as the null space projection [NSP] i.e. zero forcing of self-interference. Null space projection is basically a method of spatial suppression of the loop interference where transmit and receive antennas are spatially separated. This approach requires CSI matrix H_{r-r} and aims at reducing the LI.

The design of the W_t W_r processing filters can be done in 3 ways [25]

1. Independent design - Both the filters are designed without the knowledge of each other.

2. Separate design - Design with respect to each other [23].

3. Joint design - Design is done together.

A two-step approach [23] in the presence of the useful signal can be employed to minimize the LI. In the first stage optimal values for W_r conditioned on W_t should be found to minimize the LI thus improving reception of the useful signal. In the second stage optimal W_t conditioned on W_r can be computed to maximize the ratio of the Relay output transmit signal to the residual LI. This approach can be further augmented by the post processing hybrid scheme in [22] with the use of LMS algorithm which tries to cancel out the residual interference. As per the data reported in [24] TDC offers more isolation and supports more streams than NSP in the presence of transmit noise. With the increase in number of antennas for NSP it can support the same number of streams as TDC and can also be made immune to the Transmit noise. As characterized by [25] performance of TDC and NSP with same number of antennas is more likely to be equal given that there is no transmit noise.

Loop interference can be eliminated by precoding and decoding [49]. In the proposed scheme precoding (P) and decoding (D) matrices are selected such that

$$D^H H_{r-r} P = 0 \tag{5.5}$$

This is similar to the orthogonal scheme in [23]. Based on the efficient time slot sharing and utilization of antennas at the relay station the number of time slots can be halved (compared to half duplex relays) and full antenna gain and diversity gain can be achieved.

The performance of the conventional NSP scheme to nullify the SI can be improved by commissioning more number of transmit antennas [50] at the relay station. The increased number of Tx antennas offer increased degree of freedom while preserving the conventional precoding scheme.

Fast Forward technique in [51] attempts to maximize the SNR at the destination while maintaining the multipath delay lesser than the cyclic prefix of the OFDM framework. This ensures that there is no Inter Symbol Interference (ISI). The design incorporates a constructive pre filter in the baseband before the amplification of the signal which changes the phase of the signal for each subcarrier to sum up constructively with the LOS component at the destination as to maximize the link SNR. The experimental works have demonstrated a cancellation of 108 dB including the antenna separation isolation. A virtual antenna array can be constructed at the relay to generate virtual coupling wave path. The gain and phase of these coupling waves is changed in a manner such that it minimizes the loopback interference. Since loopback interference is contributed by the relay's transmitted signals in the past, virtual coupling paths can be implemented with FIR filters generating the cancellation waveform [93, 94]. The beamforming vector is updated on the minimum mean squared error.

Chapter 6

Mitigating the Impairment

A signal in the transmit chain before being transmitted undergoes number of impairments. Correspondingly many distortions are introduced to the receiver signals. Interference cancellation performance can be improved by modelling these parameters and by mitigating the impairments caused by them. Following are the impairments contributed by components in the Tx and Rx chains.

1. Phase noise
2. Non-linearities
3. Sampling jitter and Quantization noise by the ADC
4. IQ imaging.

Table 6.1: Impairment in Tranceivers for Self-Interference Cancellation

Phase Noise	[52],[38],[53],[54],[55],[56],[57],[58],[59],[60]
Non-Linearity	[61],[45],[38],[46],[54],[62],[63],[64],[60],[65]
IQ Imaging and Imbalance	[66],[38],[67],[54],[60]
ADC Quantization Noise & Sampling Jitter	[38],[68],[54],[60],[65]

6.1 Phase Noise

The baseband signal generated in the transmit chain is unconverted to the carrier frequency while received signal is down converted to the baseband using the local oscillator. These local oscillators are never perfect and consist of a jitter [56] reflecting in the form of the phase noise. The elimination of this phase noise plays a significant role in interference cancellation [22, 60, 62, 63, 71, 72, 73, and 74].

Ideal case of the local oscillator with a center frequency of f_c

$$y(t) = x(t)e^{j2\pi f_c t} \tag{6.1}$$

The practical case with a phase noise ϕ case can be denoted [52] by

$$y(t) = x(t)e^{(j2\pi f_c t + \phi(t))} \tag{6.2}$$

All the practical systems use free running or PLL (phase locked loop) oscillators which introduce the phase noise. This phase noise has two components namely common phase error and the inter carrier interference.

The received baseband signal by equation (1) [52] can be written as

$$y_n = [(x_n^I e^{j\phi_n^{t,I}} * h_n^I) + (x_n^s e^{j\phi_n^{t,s}} * h_n^s)]e^{j\phi_n^r} + Z_n \tag{6.3}$$

Where x_n^I, x_n^s is the interference signal and desired signal transmitted from the remote node respectively, h_n^I, h_n^s are the interference and desired signal channels respectively. $e^{j\phi_n^{t,I}}$, $e^{j\phi_n^{t,s}}$ are the phase noise terms introduced by the LO (local oscillator) in the transmit chain of the interference node and desired node while $e^{j\phi_n^r}$ is the phase noise. z_n is the receiver noise. Transforming the above equation in the frequency domain by

DFT yields the following equation5 in [52]

$$Y_k = X_k^I H_k^I J_0^c + \sum_{l=0, l\neq k}^{N-1} X_l^I H_l^I J_{k-l}^c + Y_k^s + Z_k \tag{6.4}$$

Where J_0^c is the fixed coefficient known as the common phase error [52] affecting all the subcarriers while J_{k-l}^c represents the inter carrier interference (ICI).

Phase noise can be eliminated in 2 steps [52]

1. Estimation of J_0^c and then removing it from the SI
2. Estimation of the ICI component with the MMSE estimator [59] and then its removal from the SI.

Time domain or frequency domain approach [52] can be employed for the estimation and the suppression. Time domain technique has been demonstrated to outperform the frequency domain technique by means of the complexity and the accuracy of the estimation. With an advantage of having a low noise variance for the ICI component and thus less estimation errors free running oscillates have better cancellation performance than the PLL oscillators. However based on the required complexity the improvement achieved by ICI suppression is relatively lesser.

Authors of [72, 73] have argued that the phase noise can be mitigated inherently by the analog cancellation followed by digital cancellation which attempts to cancel the phase noise causing the self-interference across the subcarriers in the OFDM scheme. But as the subcarrier spacing increases the performance of the digital cancellation [55] is limited by the phase noise. Also it has been reported that instead of using independent oscillators in the Tx and Rx chain it is favorable to share the oscillator between the two chains for the self-interference cancellation.

6.2 Non-Linearities

The baseband signal upconverted to the carrier frequency using LO is fed to the high power amplifier (PA). While in the receive chain a Low noise amplifier (LNA) is typically used to increase the strength of the incoming signal. These analog components PA and LNA introduce the intermodulation distortion in the input producing signals with non-linearities. These non linearities are the harmonics of the center frequency. If the SI at the receiver is strong then the cancellation performance is limited by these non-linearities. So it's imperative to model the non-linearities and suppress them to support the full duplex operation of the node [5, 23, 52, 55, 62, 76].

For an input x the non-linear harmonics produced can be written as

$$y(t) = \sum_{n=0}^{N-1} \alpha_n x(t)^n \tag{6.5}$$

where $x(t)$ is the analog signal in the band of interest. The equation above contains many out of band terms. The terms contributing to non-linearities in the band of interest with a little bit frequency domain analysis indicates that distortion is due to the odd power terms in the above equation. Thus above equation can be written as [5]

$$y(t) = \sum_{n=0}^{N-1} \alpha_{n+1} x(t)^{n+1} \tag{6.6}$$

Also as the order increases the power of the harmonics decreases. Thus the power of the n^{th} order harmonic [54] can be written as

$$P_{n^{th}} = P_{out} - (n-1)(IIP_n - P_{in}) \tag{6.7}$$

P_{in} is the power of the fundamental signal. While IIP_n stands for input intercept point at which the power of the harmonic is equal to the fundamental component.

As per the non-linearity model presented in [52] the non-linear distortion d_n can be written as equation (4) [23]. Higher order non-linearities are not written in the equation as the 3^{rd} order non-linearity is the most significant.

$$d_n = \alpha_3^t (x_n^I)^3 * h_n^I + \alpha_3^r (x_n^I * h_n^I + \alpha_3^t (x_n^I)^3 * h_n^I)^3 \tag{6.8}$$

α_3^t,α_3^r are transmitter and receiver non-linearities caused by the PA and the LNA respectively and h_n^I is the self-interference channel. As seen from the equation unlike the transmitter non-linearity which affects only the signal the receiver non-linearity affects the interference channel also.

Thus to mitigate the non-linearities it's essential to estimate the coefficients of the Voltera series polynomial. However the estimation is mainly inadequate given the errors in the channel estimation. Thus the joint estimation [23] of the interference channel and non-linearity coefficient should be done in the following manner

1. Rough estimate of the interference channel conditioned that mean square error is less than distortion power.

2. Construction of the interference channel and estimation of the non-linearity coefficients using the least square estimator [45].

3. Construction of the distortion signal based on the estimated coefficients.

4. Canceling the distorted signal from the received interference signal.

While analog cancellation is sufficient to suppress the fundamental component with the FIR filter, [45] has proposed a parallel Hammerstein model for the estimation of the non-linear channel, Figure 3 [45]. It has been demonstrated that the non-linear cancellation gain increases as the non-linear distortion gain increases thus allowing the

use of 10dB higher transmit power. The model for the non-linearity estimation and mitigation for the SISO case [45] can be replicated to the MIMO case while jointly modelling the non linearities induced by the cross talk.

6.3 Sampling jitter & quantization noise by the ADC

In the OFDM framework after mapping the symbols on the subcarriers by IFFT and after adding the cyclic prefix for the guard band insertion the digital baseband signal is converted to the analog domain by the DAC (Digital to Analog Converter). While at the receiver side the down converted analog baseband signal is converted to the digital using the ADC where the signal is sampled, quantized and encoded. Although the ADC is made to operate at the desired sampling frequency, there is a jitter in the sampling process thus sampling slightly off the desired frequency.

So for a sampling frequency of F_s the sampled version [68] can be represented as

$$y_n = y(nT_s + d_n) \tag{6.9}$$

Where d_n is the jitter in sampling.

As one of the weakening aspect in interference cancellation the sampling jitter needs to be estimated and compensated for. This can be done by using a reference chain. The sampling clock of the ADCs in the primary and the auxiliary receive chain can be shared. The analog baseband signal after the DAC is tapped into the ADC of the reference chain while the symbols before being mapped onto the subcarriers are tapped and fed to the reference IFFT block. Output of the Comparing the output of the ADC and the reference block gives an estimation of the jitter introduced by the sampling. Figure 1 in [68] shows the described configuration.

The jitter estimation can be done using the LS algorithms and the coefficients are set for the reference tapped to subtract it from the received interference and mitigate the effect of the sampling jitter.

At the receiver when ADC converts the analog signal to its digital domain representation, the quantization error is introduced due to rounding off of the sampled levels. Also if the self-interference is strong at the ADC input, more bits need to be dedicated for the SI signal.

The resolution of the n-bit ADC is given by

$$Resolution(dB) = n * 6.02 + 1.72$$

Where n is the number of bits, thus if the self-interference is too strong at the receiver front end it saturates the ADC of the receiver, introducing the quantization noise and leaves very few bits for the representation of the desired weak signal. This quantization noise leads to the reduced SINR at the detector [62, 77].

The quantization noise floor [68] can be calculated by

$$P_{quant} = P_{ADC} - SNR_{ADC} \tag{6.10}$$

where P_{ADC} is the input power at the ADC, SNR_{ADC} is the signal to quantization noise ratio [68] which is given by the following equation in [54]

$$SNR_{ADC} = n * 6.02 + 4.72 - PAPR \tag{6.11}$$

Where PAPR is the peak to average power ratio.

The quantization noise can be removed in 2 ways. One straight way is to use a ADC with a high resolution and large number of bits. But there is a practical limitation on the number of bits used for the resolution. Other way is to prevent the

ADC saturation by removing the SI before it reaches the ADC which can be done by the RF analog or baseband analog cancellation approach as described in the Section III.

6.4 IQ Imaging

Most of the present transceivers are using the IQ processing structures. IQ imaging arises due to the amplitude and phase mismatches between the I and Q branches (commonly known as IQ imbalance). Thus the unsatisfactory IQ mixer used in the transceivers creates the attenuated image of the signal which is represented by the following equation in [54].

$$x_{IQ}(t) = g_1 \star x(t) + g_2 \star x^*(t) \tag{6.12}$$

Here $x^*(t)$ is the image component,$\star$ denotes the convolution and $g_1(t)$, $g_2(t)$ denote the responses for the signal component and the image component.

The mixers reject the image component and it's mathematically characterized by the IRR [54] (Image Rejection Ratio)

$$IRR = 10log_{10}\left(\frac{|G_1(f)|^2}{|G_2 f(f)|^2}\right) \tag{6.13}$$

where $G_1(f)$, $G_2(f)$ are the frequency domain representations of the channel for the signal component and the image component respectively.

As analyzed in [67] the conjugate of the SI is the dominant factor in deciding SIC. The PA and LNA introduced non-linearities are created for the image component also. Equation10 in [67] shows the significance of the IQ imaging reflecting in the digital baseband at the receiver side after ADC which reduces the SINR. The 25 - 30 dB of image rejection ratio provided in the mixer is not sufficient and it leaks into the Rx chain in the interference.

Suppressing this conjugated image will lead to the improved cancellation. The developed model of widely linear digital canceller in [67] shown in Figure 2 [67] attempts the cancellation of this image caused by the IQ imaging based on the LS estimator, attempts at maximizing the SINR. The overall cancellation of 35 -50dB by widely linear digital cancellation as opposed to the 25 dB of conventional linear cancellation has been reported by the simulation experiments.

Chapter 7

A novel method for self-interference cancellation in analog domain

There are two different kinds of analog cancellers which have been developed in [5, 51] to construct the cancellation channel. The cancellation channel structure is important for the performance of the cancellation. A good cancellation channel structure is expected to have the following characteristics:

1. It has a high capacity to match an interference channel affected by wireless stutterers around the Tx and /or Rx antennas.

2. It only use reliable tunable devices.

3. It can be easily integrated with the entire radio system.

Typical RF interference channel can be written [33] as (such that$|f - f_c| < 20$ MHz)

$$h_{int,RF}(t) = \sum_{i=0}^{I-1} \alpha_i \delta(t - \tau_i - T_0) \tag{7.1}$$

Where I is the number of multipaths, α_i is the attenuation of the i^{th} path and $\tau_i + T_0$ is

the delay of i^{th} path. Let the carrier frequency be f_c and the bandwidth of interest be W. Then, the baseband equivalent of $h_{int,RF}(t)$ is

$$h_{int}(t) = e^{-j2\pi f_c T_0} \sum_{i=0}^{I-1} \alpha_i e^{-j2\pi f_c \tau_i} sinc(W(t - \tau_i - T_0)) \tag{7.2}$$

As the environment changes the values of I, α_i and τ_i also change in general although T_0 can be pre-calibrated for a given setup of Tx and Rx antennas. To be able to cancel the interference, the impulse response of the cancellation channel should be as close to the above equation as possible.

7.1 Analog Cancellation Channel Model

Figure 7.1 [33] below represents the multi-tap analog canceller structure to match the RF interference. While the internal structure [33] of a clustered c-tap has been shown in Figure 7.2. The structure of the uniform canceller is as shown as figure 1b in [33].

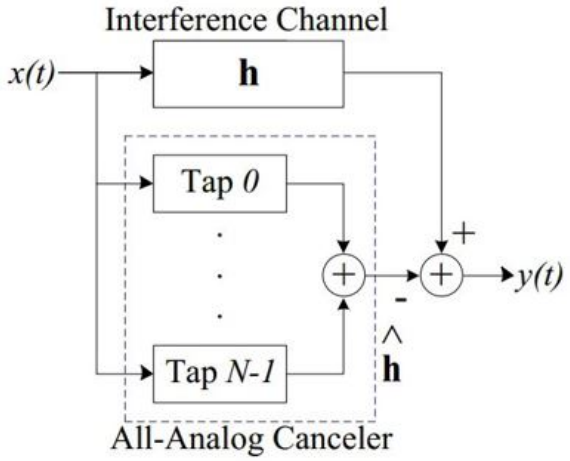

Figure 7.1: Cancellation channel and interference channel

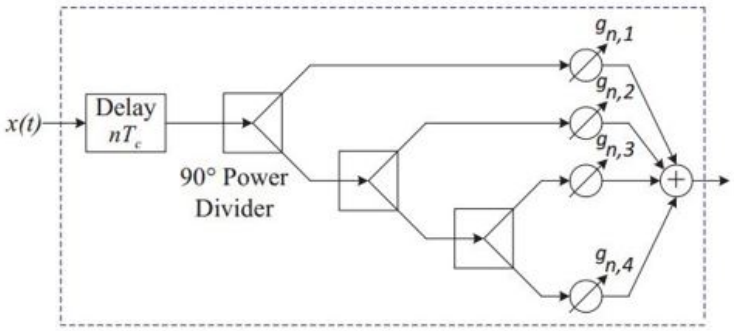

Figure 7.2: Clustered Tap Architecture

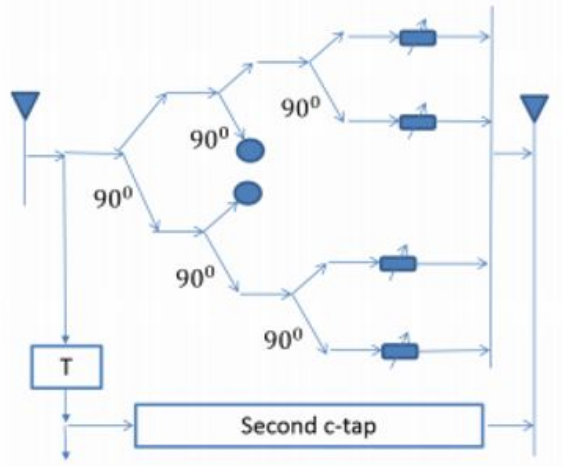

Figure 7.3: Modified clustered tap architecture [3]

As evident from the structure in Figure 7.2 the four branches are asymmetric to each other and this asymmetry will cause different insertion loss and introduce different phase offset into the 2nd, 3rd and 4th branches compared to the 1st branch. Hence to eliminate those impairments and to have uniform phase distribution, extra power splitters need to be added into the tap design and the modified structure of the c-tap is shown in Figure 7.3. The impulse response of the new structure [3] is

$$h_{can,RF}(t) = \sum_{l=0}^{N-1} \left[P_0^3 g_{l,0} + P_0^2 P_{\frac{\pi}{2}} g_{l,1} + P_0 P_{\frac{\pi}{2}}^2 g_{l,2} + P_{\frac{\pi}{2}}^3 g_{l,3} \right] \delta(t - lT - \widehat{T_0}) \qquad (7.3)$$

$g_{l,i}$represents the gain of the i^{th} attenuator and $\widehat{T_0}$ is the initial delay matched to the T_0

of the interference channel and T is the delay between two adjacent taps. While P_0 is the transfer function of the 0-degree output of a 90-degree power splitter and $P_{\frac{\pi}{2}}$ is the transfer function of the 90-degree output of the 90-degree power splitter.

And the baseband equivalent is [3]

$$h_{can}(t) = e^{-j2\pi f_c \widehat{T_0}} \sum_{l}^{N-1} P_0^3 G_l e^{-j2\pi f_c lT} sinc(W(t - lT - \widehat{T_0})) \tag{7.4}$$

Where $G_l = (g_{l.0} - g_{l,2}) + j(g_{l.3} - g_{l,1})$.

From the sampling theory [3], it is known that since $h_{int}(t)$, has the (double-sided) bandwidth W, there exist $\widehat{G_l}$ for $-\inf < l < \inf$ such that $\sum_{l=-\inf}^{\inf} \widehat{G_l} sinc(W(t - lT - \widehat{T_0}))$ with $T = \frac{1}{W}$ can match $h_{int}(t)$ exactly. But a problem with this sampling theory is that if $T = \frac{1}{W}$ then the number of required c-tap can be very large even when the delay spread is typical for a full-duplex radio with $W = 20 - 40MHz$. To reduce the number of the c-tap, to choose T as a small fraction of $\frac{1}{W}$ is suggested. Intuitively, in this way, each c-tap is effectively used to model a cluster of multipaths with a delay spread equal that fraction of $\frac{1}{W}$. The definition of bandwidth W varies according to application. Since to cancel the self-interference to the noise floor is the only consideration, the bandwidth W referred to earlier should be the bandwidth of interest at the noise floor. This could be larger than a 40dB drop bandwidth of a high power interference.

7.2 Experimental procedure and result

The experiment is based on the PHY layer analog cancellation of self-interference in full duplex communication system. The main experiment device is the commodity WARP platform.

Experimental Hardware Devices

All the required hardware devices for the experiment are as follows:

1. Keysight Network Analyzer (E5063A)
2. Agilent Spectrum analyzer (N9020A)
3. Agilent Signal Generator (N5182A)
4. PCB Analog Canceller
5. WARP kits V3 kits Virtex 6 FPGA and MAX 2829 transceivers
6. Voltage Up converters
7. High power Amplifier

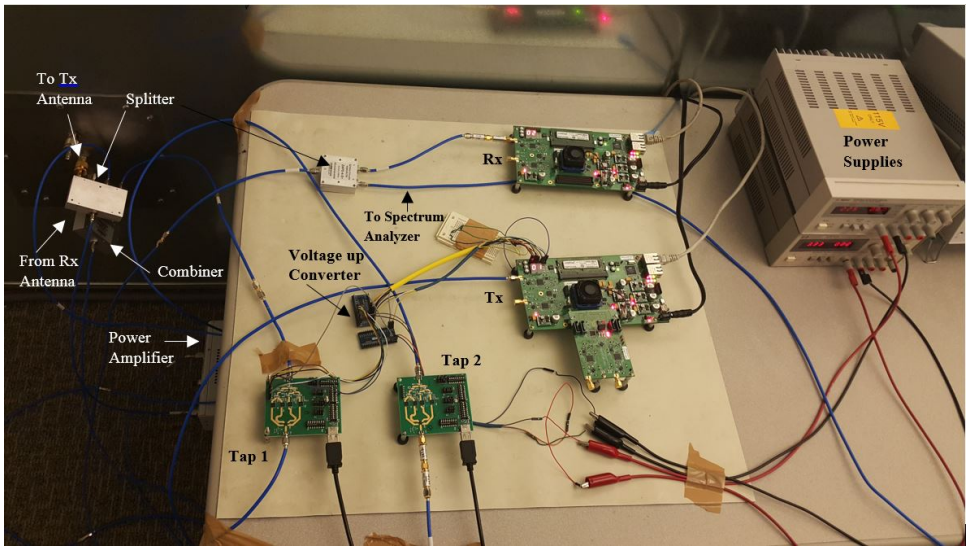

Figure 7.4: Experimental setup for RF self-interference cancellation

7.3 Result

As it is shown in the Figure 7.4, there is around 50dB difference between the RF self-interference at the radio receiver front end and the residual signal. This implies an active 50dB interference cancellation which when combined with passive mechanisms (propagation losses 25 30 dB) yield 75-80 dB of self-interference cancellation.

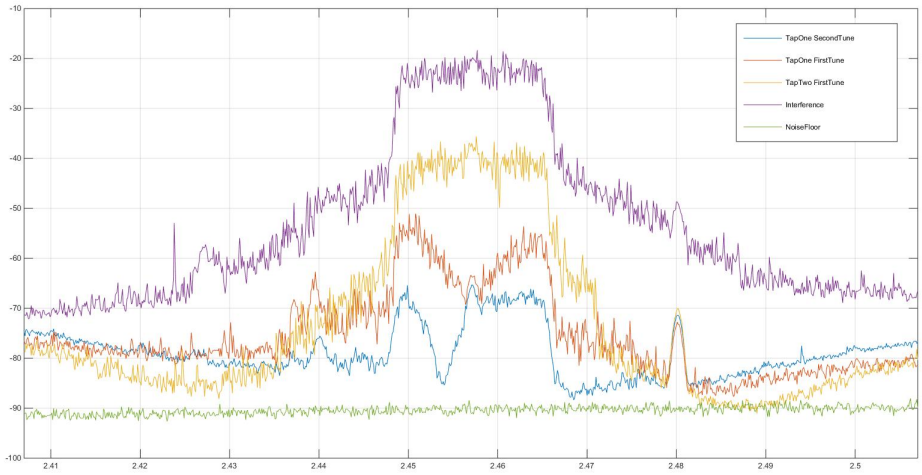

Figure 7.5: Analog Self-Interference Cancellation of 50dB by the proposed method

7.4 Conclusion

Author of [33] showed performance comparison of the uniform and clustered architecture where the latter is dependent on the choice of the carrier frequency and needs precise delay lines. Hardware experiments in [2] have shown 30 dB of cancellation and it can be ascribed to the phase dependent insertion loss of the phase shifters and attenuation dependent phase of the attenuators. As seen from the simulation results in [33] the clustered architecture has been shown to outperform the uniform architecture.

Chapter 8

Future Work

The experiment is not adaptive and there is no feedback in the process. Only the exhaustive search is automated on the hardware while the tuning the optimal values needs off-line manual involvement which will interfere the performance of the system and also makes the setting selection imprecise. Therefore, the next direction to improve the performance of the system is to develop the adaptive real-time tuning algorithms, like gradient descent, RLS and LMS.

As the result shows, the nonlinearity of the self-interference has been enhanced after the analog cancellation process and this issue has not been analyzed yet. Therefore further experimental consideration should be given to get a deeper understanding beyond this phenomenon.

Also the design should be scaled to the MIMO extension to have more degrees of freedom, diversity and to support more parallel streams to enhance the throughput.

Chapter 9

Conclusion

Analog cancellation complemented with the digital cancellation and antenna cancellation can theoretically push the strong self-interference to the receiver noise floor and thus double or nearly double the throughput of the communication system. The performance of this full duplex system is critically impacted by various parameters and components and thus a careful consideration and the robust algorithm development is needed for the reliable full duplex operation to be commercialized.

Realizing the novel structure of the cancellation tap, around 50dB of analog domain cancellation of the self-interference has been demonstrated. So far, the result of the experiments show the sub-optimal performance, characteristics and the capabilities of this novel approach. The result points out that in the near future, the promising and achievable full duplex can replace the existing half duplex radios.

Part II

LTE-Unlicensed

Chapter 10

Introduction

Last decade has seen an unprecedented increase in demands and usage of wireless data and voice services. Escorting this drift is the development of smart phones with a far deeper market penetration. To cope up with the demand of service and providing QoS with limited resources various mobile carriers and modem companies started exploring for further improvements with an aim of efficient resource utilization and robust techniques. This strategizing led to the establishment of a 3GPP standardization committee in 1998 with 400 members. 3GPP encompassed standards such as GSM, GPRS, EDGE, UMTS, HSPA until 2004.

With various requirements such as

- Voice over IP
- Higher peak data rates up to 100Mbps
- Low power efficiency
- High capacity and frequency usage flexibility
- Improved system architecture

3GPP started investigating 4^{th} generation LTE (Long term evolution) and it was later standardized under the Release-8 3GPP with supporting 2 modes as FDD and TDD providing 100 Mbps downlink throughput for LTE Cat 3 UE (User equipment).

Enhancement

With an aim to increase the throughput up to 1Gbps, LTE Advanced was standardized by 3GPP under Release- 10.

Following are the additional features of LTE Advanced compared to LTE

- Carrier Aggregation - Supporting multiple carriers.
- Coordinated Multi Point - Coordination of LTE base stations to improve performance at the cell edge.
- LTE relaying - Forwarding of signals from remote base stations to main base station.
- LTE device to device - Emergency based device to device communication facility.

Chapter 11

LTE

11.1 Introduction

LTE stands for Long Term Evolution and is marketed as 4G under current cellular markets. LTE provides enhanced throughput compared with previously established standards such as GSM, HSPA, etc. LTE is mainly composed of 2 constituents namely UE (User Equipment) - end user device and eNodeB - Cellular Base Station. The air interface between eNodeB and UE is Uu which supports high data rate because of the underlying OFDMA (Orthogonal Frequency Division Multiple Access) method in the downlink while SC-FDMA (Single Carrier- Frequency Division Multiple Access) is used in the uplink.

11.2 LTE Parameters

LTE uses a frame structure for uplink and downlink transmission [4]. Each frame consists of a resource grid which carries different channels and pertaining data.

Frame duration - 10ms

Number of sub frames - 10

Number of slots in a frame - 20

Number of slots in a sub frame - 2

Sub frame duration - 1ms

Slot duration - 0.5ms

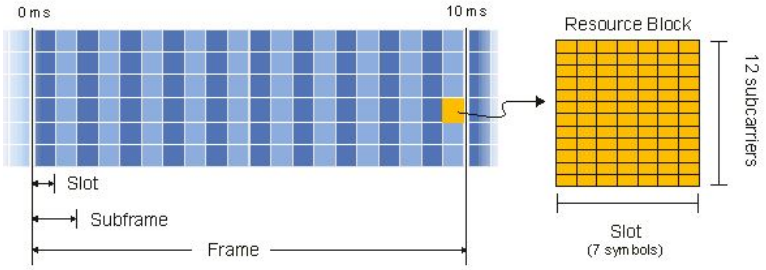

Figure 11.1: LTE frame structure [4]

11.3 LTE Frame Types

LTE supports 2 types of frames configurations - FDD and TDD

Type 1 FDD

In this mode, downlink and uplink frames are 10ms long and they differ from each other in frequency. For full duplex FDD LTE mode, these both frames are transmitted continuously and in synchronization.

Type 2 TDD

In this mode, downlink and uplink frames are transmitted on the same frequency but are multiplex in the time. Based on the standard there are 7 possible configurations of the TDD Frame and these configurations specify the location of downlink,

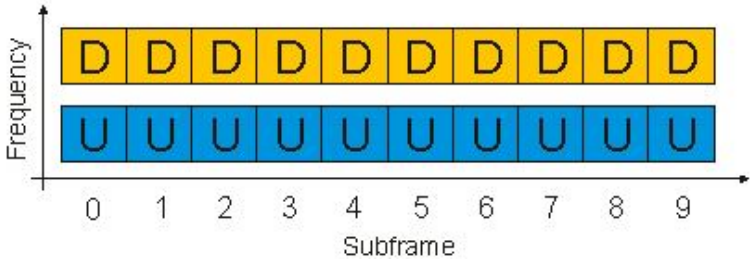

Figure 11.2: LTE FDD frame structure [4]

uplink and special subframes.

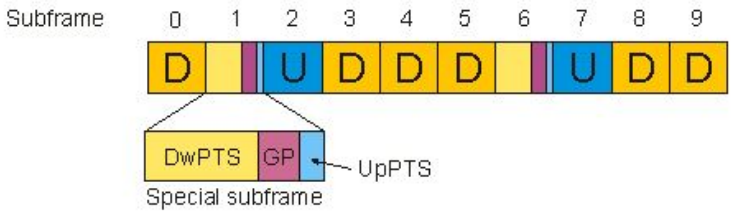

Figure 11.3: LTE TDD frame structure(Configuration-2)[4]

Speical Subframe - Used for switching between downlink and uplink and they contain DwPTS, GP and UpPTS.

DwPTS - Downlink pilot Time Slot. Contains P-SS (Primary Synchronization Signal) and may contain PDSCH (Physical Downlink Shared Channel).

GP - Guard period. Used for seperating DwPTS and UpPTS. Nothing is transmitted during this period.

UpPTS - Uplink Pilot Time Slot. Contains SRS (Sounding Reference Singal) and PRACH (Physical Random Access Channel).

11.4 LTE Features

Downlink Access Method - OFDMA.

Uplink Access Method - SC- FDMA.

Subcarrier mapping - Localized.

Modulation Schemes - BPSK, QPSK, 16 QAM, 64 QAM.

Subcarrier spacing - 15KHz.

Channel Coding - Convolutional coding and Turbo Coding.

MIMO mode - 2/4 Tx and 2/4 RX.

Table 11.1: LTE BW vs RB configuration [4]

Bandwidth (MHz)	Resource Blocks	Subcarriers in DL	Subcarriers in UL	IFFT/FFT point
1.4	6	73	72	128
3	15	181	180	256
5	25	301	300	512
10	50	601	600	1024
15	75	901	900	1536
20	100	1201	1200	2048

11.5 LTE UE Catagories

LTE UE categories specify different physical layer parameters such as modulation schemes, MIMO, No. of MCH bits, data rate, buffer size, etc. Description of it can be found under the Rel-10 LTE 3GPP standard.

11.6 LTE Physical Layer

LTE uses Orthogonal Frequency Division Multiple Access (OFDMA) [5] in the downlink. OFDMA combats frequency selective fading and transforms a wideband channel into flat fading channel for narrow band subcarriers. Single Carrier - Frequency Division Multiple Access (SC-FDMA) is used in the uplink as OFDMA has a high Peak to Average Power Ratio. In OFDMA, multiple symbols are transmitted on multiple carriers at the same time in parallel. While in SC-FDMA, a single symbol is transmitted on a single carrier in a serial fashion. This intuitively yields higher throughput in the downlink direction. Following is the block diagram for SC-FDMA and OFDMA mappers. The only difference in them is the use of DFT (Discrete Fourier Transform) in the SC-FDMA chain.

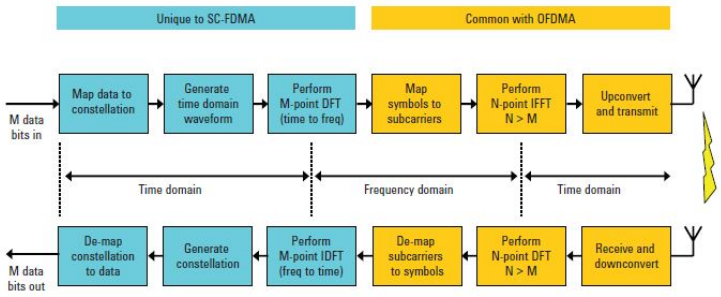

Figure 11.4: SC-FDMA and OFDMA signal baseband and reception [5]

Following are the steps involved in LTE downlink baseband signal generation. [4]

1. Scrambling of the coded bits in the code word.

2. Modulation of the scrambled bits.

3. Mapping of complex modulated symbols on the transmission layers.

4. Precoding of the complex symbols for different antenna ports.

5. Mapping of pre-coded complex symbols onto resource elements in resource grid.

6. Generation of the complex time domain OFDMA waveform.

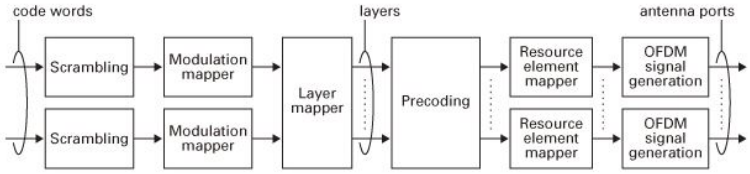

Figure 11.5: LTE downlink baseband signal generation [5]

Following are the steps involved in the LTE uplink baseband signal generation. [4]

1. Scrambling of the coded bits in the code word.

2. Modulation of the scrambled bits.

3. Precoding of the complex symbols for different antenna ports.

4. Mapping of pre-coded complex symbols onto resource elements in resource grid.

5. Generation of the complex time domain SC-FDMA waveform.

Figure 11.6: LTE uplink baseband signal generation [5]

11.7 LTE Signals and Channels

11.7.1 Signals

P-SS: Primary Synchronization Signal. Present in downlink at 6th symbol of slot 0 and slot 10. Central 72 subcarriers are used and is made up of Zadoff Chu sequence of length 63. Useful for subframe level synchronization of UE, slot timing detection and Physical layer ID detection.

S-SS: Secondary Synchronization Signal. Present in downlink at 5th symbol of slot 0 and slot 10. Central 72 subcarriers are used and is made up of BPSK modulated 31 length sequence. Used for radio frame timing detection, Physical layer cell ID detection and to determine TDD or FDD.

RS: Reference signal. Present in downlink and modulated using QPSK. Present in 1st and 4th symbol in each time slot. Used for channel estimation at the UE end.

DM-RS: Demodulation reference signal. Present in 4th symbol. Used for channel estimation at the eNodeB end.

SRS: Sounding reference signal. Present in uplink and mapped on last symbol of every subframe. Modulated using Zadoff Chu sequence and is used for channel estimation.

11.7.2 Physical Channels

PBCH: Physical Broadcast channel. Downlink. Modulated using QPSK and coding rate of $\frac{1}{2}$ and mapped on central 72 subcarriers. Detectable without prior knowledge and is

present in the Master Information Block (MIB). Transmission is spread over 4 frames. Carries information such as parameters essential for intital cell access, downlink bandwidth, HARQ indicator and 8 MSB of the system frame number (SFN).

PDSCH: Physical downlink shared channel. Used for carrying user data. Paging and system information blocks (SIB) may be transmitted over PDSCH. Modulation schemes can be QPSK, 16 QAM or 64 QAM.

PDCCH: Physical downlink control channel. Present in 1st to 4th symbols of the subframe. Used to carry downlink control information (DCI). Modulated using QPSK. Conveys UE about the resource allocation, modulation scheme, and coding and HARQ information.

PCFICH: Physical control format indicator channel. Downlink. Present in the 1st symbol of every subframe. Informs UE about the number of symbols used for PDCCH.

PRACH: Physical random access channel. Present in uplink and carries random access preambles used in the LTE random access procedure initiation to enter the network. Consists of 72 subcarriers. The random access preamble uses 839 subcarriers with a spacing of 1.25 KHz and a guard band of 15 KHz on both the sides. Total of 64 RACH sequences have been standardized under 3GPP.

PUSCH: Physical uplink shared channel. Carries uplink control information (UCI), user data and signaling messages. Modulation of QPSK, 16 QAM or 64 QAM can be used.

PUCCH: Physical uplink control channel. Carries uplink control information (UCI), channel quality indicator (CQI), HARQ ACK/NACK and MIMO feedback. BPSK or QPSK modulation can be used. Uses 2 RBs, one at the one end of the system while other at the diagonally opposite end in the next time slot.

11.8 LTE Transmission modes

Various transmission modes [4] relating to transmit diversity and space division multiplexing have been specified under Rel-8 3GPP to enhance the quality of the reception and to improve the throughput depending on the SISO or MIMO transmission.

Table 11.2: LTE Transmission Modes

LTE Transmission Mode	**Description**
1	Single Antenna transmission and Reception
2	Transmit diversity
3	Open loop codebook based precoding
4	Closed loop codebook based precoding
5	Multi user MIMO
6	Single layer codebook based precoding
7	Single layer beamforming non codebook based precoding
8	Up to 2 layers non codebook based precoding
9	Up to 8 layers non codebook based precoding

Chapter 12

Carrier aggregation and LTE Unlicensed

12.1 Carrier Aggregation

LTE Rel-8 uses channel bandwidths of 1.4, 3, 5, 10, 15 and 20 MHz for transmission with the use of a single carrier in the allocated frequency band [4].

LTE advanced offers significantly higher data throughput. In order to achieve this throughput, it is essential to have a larger transmission bandwidth for supported carriers. So the method of using multiple single carriers for transmission thus allocating more bandwidth to the end user is termed as carrier aggregation. These aggregated carriers are either contiguous or non- contiguous with the max number of total carriers up to 5 so providing 100MHz (20MHz X 5) of the spectrum. Rel-10 supports the backward computability with Rel-8 and Rel-9 UEs [4] [69].

12.1.1 Types of carrier aggregation (Figure 12.1

1. Intra band contiguous
2. Intra band non contiguous
3. Inter band non contiguous

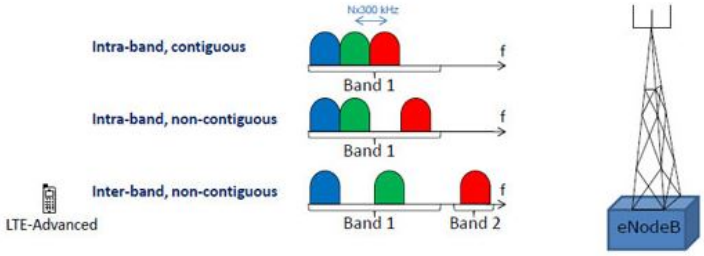

Figure 12.1: Types of carrier aggregation [4]

12.1.2 LTE Aggregated carriers

There are 2 types of aggregated carriers [4].

- Primary component carrier - Main carrier in the group. There is a primary downlink and an associated uplink primary carrier.
- Secondary component carrier - There may be up to 5 secondary component carriers.

The configuration of the primary carrier is terminal specific and association between downlink and uplink primary carrier is cell specific.

12.1.3 Carrier Aggregation in TDD

In LTE TDD mode number of component carriers and their bandwidths are the same for both uplink and downlink direction. Also # of UL (CC) <= # of DL (CC)

12.1.4 Carrier Aggregation in FDD

In LTE FDD mode number of component carriers in uplink and downlink and their bandwidths may differ.

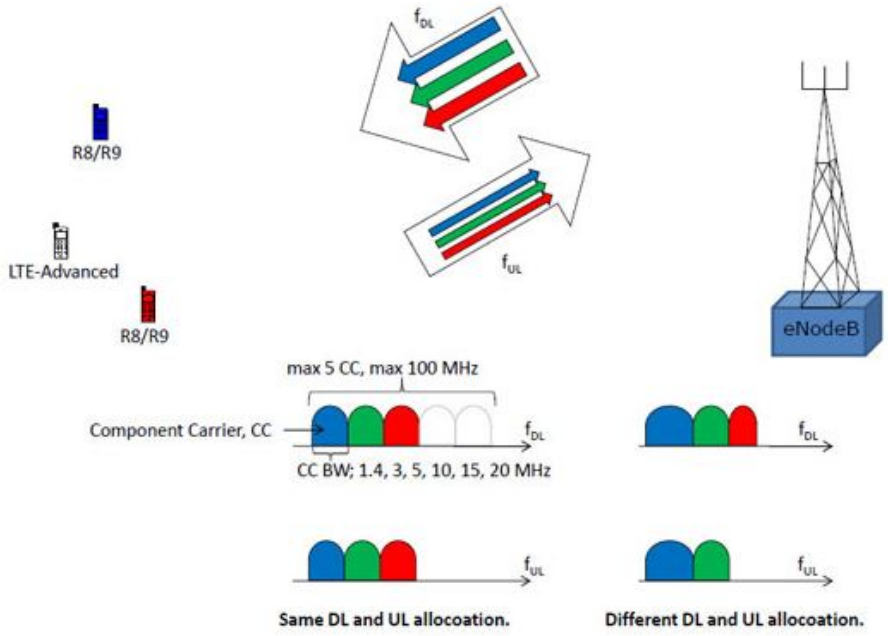

Figure 12.2: Carrier aggregation in FDD Mode [4]

12.2 LTE Unlicensed (LTE-U) and LTE- Licensed Assisted Access (LTE-LAA)

Currently deployed LTE networks are carrying enormous amount of data in the limited spectrum approved by the FCC. There is a vast amount of unlicensed spectrum present in the ISM (Industrial, Scientific and Medical) bands at 2.4GHz and 5GHz. 5GHz band is considerably less populated compared to 2.4GHz. Hence 5GHz is a band of interest for LTE-LAA/ LTE-U.

The 3GPP committee has established the LTE-U forum [70] for the developments and standardization of LTE-U under Rel-13. Many industrials participants such as Verizon, Alcatel-Lucent, Ericsson, and Qualcomm are the founding members of this forum.

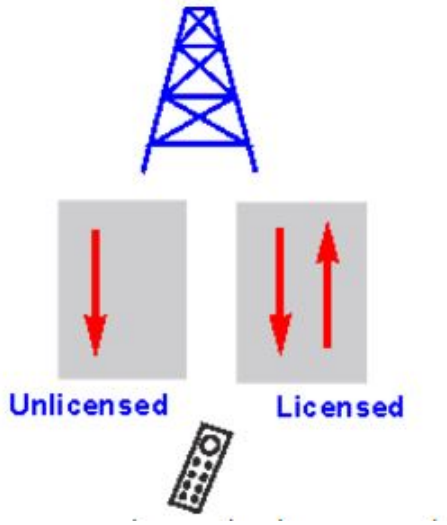

Figure 12.3: LTE - Unlicensed [6]

LTE-U delivers the gains of LTE-Advanced to the unlicensed spectrum, letting cellular carriers to carry the data traffic onto the unlicensed frequencies present in the UNII-1 and UNII-3 band. So LTE-U is basically inter band carrier aggregation. But there is a major obligation to coexist with the users of the 5GHz band (Wi-Fi) - to perform channel assessment and to be channel aware. Also there will be just the downlink in the unlicensed band assisted by the licensed band link [71].

12.2.1 LTE-U vs LTE - LAA

LTE-U: Employs carrier sense adaptive transmission to sense the channel activity for the presence of Wi-Fi and to determine the channel utilization function [71]. LTE on off

duty cycling is done based on the calculation of channel utilization. Maximum continuous on time is 50 msec. It has been considered for deployments in USA, Kora, India, etc.

LTE-LAA: Employs Listen before Talk (LBT) as used in the IEEE WLAN systems for gaining access to the wireless channel [71]. Clear channel assessment is performed under LBT to start the LTE transmission. Maximum continuous on time is 4msec. It has been considered for deployments in Europe, Japan and etc.

12.3 LTE- Wi-Fi Coexistence

Since LTE-LAA will be sharing the spectrum with Wi-Fi, an aggressive access of the spectrum will lead to collisions and both LTE and Wi-Fi will witness a drop in throughput. So LTE has to coexist with Wi-Fi peacefully so not to hamper its operation and be flexible towards the spectrum access. So LTE employs the Listen before Talk method adopted by the Wi-Fi to gain channel access where the transmitting terminal listens to the channel for a specified time and starts the transmission if channel is unoccupied [71]. So LTE will vary its operation in the 5GHz band based on the Wi-Fi activity.

Clear channel assessment is performed in 2 steps by Wi-Fi terminals-

CCA-ED(Energy detect): Wi-Fi terminals sense the energy in the channel and back off from transmission if the channel is occupied. The ED threshold is generally 20dB above the receiver sensitivity and is around -62dBm for 802.11 WLAN systems. If the sensed energy is above then the ED threshold then transmission is held back.

CCA-CS(Carrier Sense): The WLAN receiver detects and decodes the fixed format Wi-Fi preamble based on correlation. From this decoding information about the duration

for which the channel will be occupied by the ongoing transmission is inferred from the Network Allocation Vector present in the duration field of the MAC header.

Hence the LTE eNodeB performs clear channel assessment similar to Wi-Fi to gain the understanding of the channel. Also with the decoding of Wi-Fi beacons in actions arriving at periodical intervals, information about number of Wi-Fi access points and relevant parameters is obtained to create a channel map.

So the LTE eNodeB adaptively gains the channel access and extracts the information with decoding of beacons. The algorithm running in eNodeB replicates the entire WLAN receiver chain consisting of following modules -

1. Timing offset estimation and compensation from STS (Short Training sequence) and LTS (Long Training sequence).
2. Frequency offset estimation and compensation.
3. Channel estimation.
4. Validating the MCS used for the SIG symbol in the PHY header and obtaining information about packet size and modulation scheme and coding rate used.
5. Removing Cyclic prefix, performing FFT and compensating the channel with channel estimate.
6. Demodulation.
7. De-interleaving.
8. Decoding.
9. Descrambling and performing the CRC check.

12.4 Hardware Implementation

A real time implementation of Pre-release 13 LTE-LAA was demonstrated at Intel developer forum in San Francisco and Globecom, San Diego.

Following were the various equipment used in the demo -

1. Intel T3300 small cell eNodeB with 2 Arm A9 cores and 4 CEVA XC323 DSP cores.

2. Intel Cat-5 UE 7260 supporting carrier aggregation supporting downlink data rate of 300Mbps.

3. Dual band 802.11n/ac WLAN Access Point (AP).

4. 802.11n/ac capable Wi-Fi STA (Laptop, smart phone).

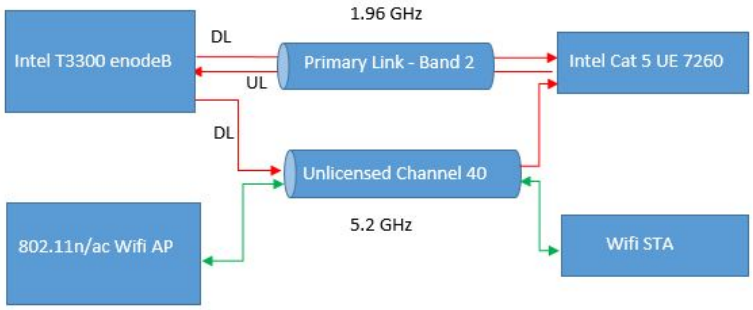

Figure 12.4: Pre-Release 13 LTE-LAA Hardware demo block diagram

WLAN channel used was channel 40 at 5.2GHz. The WLAN link used was 802.11n 2 spatial streams with 20MHz channel providing peak data rate of 144.2 Mbps. All the demonstrations were carried out in a cabled environment because of the requirement of keeping radiation levels as low as possible.

It was demonstrated that LTE eNodeB can coexist peacefully with the Wi-Fi and can share the spectrum fairly. UDP traffic and an open source HD video was pushed from Wi-Fi AP to Wi-Fi STA while adaptive UDP traffic was pushed from LTE eNodeB to LTE UE.

Chapter 13

Conclusions

Many supports of the LTE-LAA/LTE-U have demonstrated a fair coexistence between Wi-Fi and LTE in the unlicensed spectrum. The results [70] have shown that LTE can enhance its throughput dynamically by using a supplemental downlink in the 5GHz band without hampering Wi-Fi throughput and operation.

However some industry experts have shown LTE to be a poor neighbor to the Wi-Fi. Hence it is essential to identify the bottlenecks and challenges in channel access procedures and necessary precautions should be included in the system level implementation to develop a friendly eco system in the unlicensed band.

From a device point of view, as today's mobile phones house a powerful processors it is essential to identify the burden incurred to support the LTE-U operation. Also at the eNodeB it is essential to recognize the burden experienced to support the implementation of complicated algorithms for channel access procedures and transmission.

Bibliography

[1] Dinesh Bharadia, Emily McMilin, and Sachin Katti. Full duplex radios. In *ACM SIGCOMM Computer Communication Review*, volume 43, pages 375–386. ACM, 2013.

[2] J.G. McMichael and K.E. Kolodziej. Optimal tuning of analog self-interference cancellers for full-duplex wireless communication. In *Communication, Control, and Computing (Allerton), 2012 50th Annual Allerton Conference on*, pages 246–251, Oct 2012.

[3] Yingbo Hua, Yifan Li, C. Mauskar, and Qiping Zhu. Blind digital tuning for interference cancellation in full-duplex radio. In *Signals, Systems and Computers, 2014 48th Asilomar Conference on*, pages 1691–1695, Nov 2014.

[4] A Global Initiative 3GPP. http://www.3gpp.org/.

[5] http://cp.literature.agilent.com/litweb/pdf/5989-8139en.pdf.

[6] www.radio-electronics.com/info/cellulartelecomms/lte-long-term-evoultion/lte-u-unlicensed-laa-license-assisted-access.php.

[7] S. Chen, M.A. Beach, and J.P. McGeehan. Division-free duplex for wireless applications. *Electronics Letters*, 34(2):147–148, Jan 1998.

[8] H. Hamazumi, K. Imamura, N. Iai, K. Shibuya, and M. Sasaki. A study of a loop interference canceller for the relay stations in an sfn for digital terrestrial broadcasting. In *Global Telecommunications Conference, 2000. GLOBECOM '00. IEEE*, volume 1, pages 167–171 vol.1, 2000.

[9] B. Radunovic, D. Gunawardena, P. Key, A. Proutiere, N. Singh, V. Balan, and G. Dejean. Rethinking indoor wireless mesh design: Low power, low frequency, full-duplex. In *Wireless Mesh Networks (WIMESH 2010), 2010 Fifth IEEE Workshop on*, pages 1–6, June 2010.

[10] E. Everett, A. Sahai, and A. Sabharwal. Passive self-interference suppression for full-duplex infrastructure nodes. *Wireless Communications, IEEE Transactions on*, 13(2):680–694, February 2014.

[11] Jung Il Choi, Mayank Jain, Kannan Srinivasan, Philip Levis, and Sachin Katti. Achieving Single Channel, Full Duplex Wireless Communication. In *Proceedings of the 16th Annual International Conference on Mobile Computing and Networking (Mobicom 2010)*, September 2010.

[12] S. Rangarajan X. Zhang M. A. Khojastepour, K. Sundaresan and S. Barghi. The case for antenna cancellation for scalable full duplex wireless communications. Hotnets, Nov 2011.

[13] G. Patel A. Sahai and A. Sabharwal. Pushing the limits of full-duplex: Design and real- time implementation. Jul 2011.

[14] Bo Chen, Vivek Yenamandra, and Kannan Srinivasan. Flexradio: Fully flexible radios and networks. In *12th USENIX Symposium on Networked Systems Design and Implementation (NSDI 15)*, pages 205–218, Oakland, CA, May 2015. USENIX Association.

[15] Aimin Tang and Xudong Wang. Balanced rf-circuit based self-interference cancellation for full duplex communications. *Ad Hoc Networks*, 24, Part A:214 – 227, 2015.

[16] E. Foroozanfard, O. Franek, A. Tatomirescu, E. Tsakalaki, E. De Carvalho, and G.F. Pedersen. Full-duplex mimo system based on antenna cancellation technique. *Electronics Letters*, 50(16):1116–1117, July 2014.

[17] E. de Carvalho E. Tsakalaki, E. Foroozanfard and G. F. Pedersen. A2-order mimo full-duplex antenna system. In *Antennas and Propagation (EuCAP), 2010 Proceedings of the Fourth European Conference on*, pages 2546–2550, April 2014.

[18] B. Debaillie, D.-J. van den Broek, C. Lavin, B. van Liempd, E.A.M. Klumperink, C. Palacios, J. Craninckx, B. Nauta, and A. Parssinen. Analog/rf solutions enabling compact full-duplex radios. *Selected Areas in Communications, IEEE Journal on*, 32(9):1662–1673, Sept 2014.

[19] B. van Liempd, B. Debaillie, J. Craninckx, C. Lavin, C. Palacios, S. Malotaux, J.R. Long, D.J. van den Broek, and E.A.M. Klumperink. Rf self-interference cancellation for full-duplex. In *Cognitive Radio Oriented Wireless Networks and Communications (CROWNCOM), 2014 9th International Conference on*, pages 526–531, June 2014.

[20] E. Ahmed, A.M. Eltawil, Zhouyuan Li, and B.A. Cetiner. Full-duplex systems using multireconfigurable antennas. *Wireless Communications, IEEE Transactions on*, 14(11):5971–5983, Nov 2015.

[21] E. Everett, M. Duarte, C. Dick, and A. Sabharwal. Empowering full-duplex wireless communication by exploiting directional diversity. In *Signals, Systems and Computers (ASILOMAR), 2011 Conference Record of the Forty Fifth Asilomar Conference on*, pages 2002–2006, Nov 2011.

[22] Byungjin Chun, Eui-Rim Jeong, Jingon Joung, Yukyung Oh, and Yong H Lee. Pre-nulling for self-interference suppression in full-duplex relays. In *Proceedings: APSIPA ASC 2009: Asia-Pacific Signal and Information Processing Association, 2009 Annual Summit and Conference*, pages 91–97. Asia-Pacific Signal and Information Processing Association, 2009 Annual Summit and Conference, International Organizing Committee, 2009.

[23] P. Lioliou, M. Viberg, M. Coldrey, and F. Athley. Self-interference suppression in full-duplex mimo relays. In *Signals, Systems and Computers (ASILOMAR), 2010*

Conference Record of the Forty Fourth Asilomar Conference on, pages 658–662, Nov 2010.

[24] T. Riihonen, S. Werner, and R. Wichman. Residual self-interference in full-duplex mimo relays after null-space projection and cancellation. In *Signals, Systems and Computers (ASILOMAR), 2010 Conference Record of the Forty Fourth Asilomar Conference on*, pages 653–657, Nov 2010.

[25] T. Riihonen, S. Werner, and R. Wichman. Mitigation of loopback self-interference in full-duplex mimo relays. *Signal Processing, IEEE Transactions on*, 59(12):5983–5993, Dec 2011.

[26] L. Laughlin, M.A. Beach, K.A. Morris, and J.L. Haine. Optimum single antenna full duplex using hybrid junctions. *Selected Areas in Communications, IEEE Journal on*, 32(9):1653–1661, Sept 2014.

[27] M.E. Knox. Single antenna full duplex communications using a common carrier. In *Wireless and Microwave Technology Conference (WAMICON), 2012 IEEE 13th Annual*, pages 1–6, April 2012.

[28] Steven S Hong, Jeffrey Mehlman, and Sachin Katti. Picasso: flexible rf and spectrum slicing. *ACM SIGCOMM Computer Communication Review*, 42(4):37–48, 2012.

[29] Melissa Duarte, Chris Dick, and Ashutosh Sabharwal. Experiment-driven characterization of full-duplex wireless systems. *Wireless Communications, IEEE Transactions on*, 11(12):4296–4307, 2012.

[30] John R Krier and Ian F Akyildiz. Active self-interference cancellation of passband signals using gradient descent. In *PIMRC*, pages 1212–1216, 2013.

[31] R. Askar, T. Kaiser, B. Schubert, T. Haustein, and W. Keusgen. Active self-interference cancellation mechanism for full-duplex wireless transceivers. In *Cognitive Radio Oriented Wireless Networks and Communications (CROWNCOM), 2014 9th International Conference on*, pages 539–544, June 2014.

[32] Mayank Jain, Jung Il Choi, Taemin Kim, Dinesh Bharadia, Siddharth Seth, Kannan Srinivasan, Philip Levis, Sachin Katti, and Prasun Sinha. Practical, real-time, full duplex wireless. In *Proceedings of the 17th annual international conference on Mobile computing and networking*, pages 301–312. ACM, 2011.

[33] A. Gholian, Yiming Ma, and Yingbo Hua. A numerical investigation of all-analog radio self-interference cancellation. In *Signal Processing Advances in Wireless Communications (SPAWC), 2014 IEEE 15th International Workshop on*, pages 459–463, June 2014.

[34] Yingbo Hua, Yiming Ma, Armen Gholian, Yifan Li, Ali Cagatay Cirik, and Ping Liang. Radio self-interference cancellation by transmit beamforming, all-analog cancellation and blind digital tuning. *Signal Process.*, 108(C):322–340, March 2015.

[35] Jong-Ho Lee. Self-interference cancelation using phase rotation in full-duplex wireless. *Vehicular Technology, IEEE Transactions on*, 62(9):4421–4429, Nov 2013.

[36] Yingbo Hua, Yiming Ma, Ping Liang, and A. Cirik. Breaking the barrier of transmission noise in full-duplex radio. In *Military Communications Conference, MILCOM 2013 - 2013 IEEE*, pages 1558–1563, Nov 2013.

[37] B. Kaufman, J. Lilleberg, and B. Aazhang. An analog baseband approach for designing full-duplex radios. In *Signals, Systems and Computers, 2013 Asilomar Conference on*, pages 987–991, Nov 2013.

[38] E. Ahmed and A.M. Eltawil. All-digital self-interference cancellation technique for full-duplex systems. *Wireless Communications, IEEE Transactions on*, 14(7):3519–3532, July 2015.

[39] S. Enserink, M.P. Fitz, K. Goverdhanam, Changyi Gu, T.R. Halford, I. Hossain, G. Karawasy, and O.Y. Takeshita. Joint analog and digital interference cancellation. In *Microwave Symposium (IMS), 2014 IEEE MTT-S International*, pages 1–3, June 2014.

[40] Shenghong Li and R.D. Murch. Full-duplex wireless communication using transmitter output based echo cancellation. In *Global Telecommunications Conference (GLOBECOM 2011), 2011 IEEE*, pages 1–5, Dec 2011.

[41] Micael Bernhardt, Fernando H Gregorio, and Juan E Cousseau. A robust wireless ofdm echo cancellation system. *XV Reunin de Trabajo en Procesamiento de la Informacin y Control, RPIC*, 2013.

[42] S.E. Johnston and P.D. Fiore. Full-duplex communication via adaptive nulling. In *Signals, Systems and Computers, 2013 Asilomar Conference on*, pages 1628–1631, Nov 2013.

[43] Ehsan Aryafar, Mohammad Amir Khojastepour, Karthikeyan Sundaresan, Sampath Rangarajan, and Mung Chiang. Midu: Enabling mimo full duplex. In *Proceedings of the 18th Annual International Conference on Mobile Computing and Networking*, Mobicom '12, pages 257–268, New York, NY, USA, 2012. ACM.

[44] A. Balatsoukas-Stimming, P. Belanovic, K. Alexandris, and A. Burg. On self-interference suppression methods for low-complexity full-duplex mimo. In *Signals, Systems and Computers, 2013 Asilomar Conference on*, pages 992–997, Nov 2013.

[45] L. Anttila, D. Korpi, V. Syrjala, and M. Valkama. Cancellation of power amplifier induced nonlinear self-interference in full-duplex transceivers. In *Signals, Systems and Computers, 2013 Asilomar Conference on*, pages 1193–1198, Nov 2013.

[46] L. Anttila, D. Korpi, E. Antonio-Rodriguez, R. Wichman, and M. Valkama. Modeling and efficient cancellation of nonlinear self-interference in mimo full-duplex transceivers. In *Globecom Workshops (GC Wkshps), 2014*, pages 777–783, Dec 2014.

[47] D. Korpi, L. Anttila, and M. Valkama. Reference receiver based digital self-interference cancellation in mimo full-duplex transceivers. In *Globecom Workshops (GC Wkshps), 2014*, pages 1001–1007, Dec 2014.

[48] Dinesh Bharadia and Sachin Katti. Full duplex mimo radios. In *11th USENIX Symposium on Networked Systems Design and Implementation (NSDI 14)*, pages 359–372, Seattle, WA, April 2014. USENIX Association.

[49] Hyungsik Ju, Eunsung Oh, and Daesik Hong. Improving efficiency of resource usage in two-hop full duplex relay systems based on resource sharing and interference cancellation. *Wireless Communications, IEEE Transactions on*, 8(8):3933–3938, August 2009.

[50] Byungjin Chun and Yong H. Lee. A spatial self-interference nullification method for full duplex amplify-and-forward mimo relays. In *Wireless Communications and Networking Conference (WCNC), 2010 IEEE*, pages 1–6, April 2010.

[51] S. Katti Bharadia, K. R. Joshi. Fastforward: fast and constructive full duplex relays. pages 199–210. ACM, 2014.

[52] E. Ahmed and A.M. Eltawil. On phase noise suppression in full-duplex systems. *Wireless Communications, IEEE Transactions on*, 14(3):1237–1251, March 2015.

[53] Ville Syrjaelae and Koji Yamamoto. Self-interference cancellation in full-duplex radio transceivers with oscillator phase noise. In *European Wireless 2014; 20th European Wireless Conference; Proceedings of*, pages 1–6, May 2014.

[54] Mikko Valkama Dani Korpi, Lauri Anttila. Feasibility of in-band full-duplex radio transceivers with imperfect rf components: Analysis and enhanced cancellation algorithms. *CoRR*, abs/1409.1365, 2014.

[55] Shihai Shao, Xin Quan, Ying Shen, and Youxi Tang. Effect of phase noise on digital self-interference cancellation in wireless full duplex. In *Acoustics, Speech and Signal Processing (ICASSP), 2014 IEEE International Conference on*, pages 2759–2763, May 2014.

[56] A. Sahai, G. Patel, C. Dick, and A. Sabharwal. On the impact of phase noise on active cancelation in wireless full-duplex. *Vehicular Technology, IEEE Transactions on*, 62(9):4494–4510, Nov 2013.

[57] V. Syrjala, K. Yamamoto, and M. Valkama. Analysis and design specifications for full-duplex radio transceivers under rf oscillator phase-noise with arbitrary spectral shape. *Vehicular Technology, IEEE Transactions on*, PP(99):1–1, 2015.

[58] V. Syrjala, M. Valkama, L. Anttila, T. Riihonen, and D. Korpi. Analysis of oscillator phase-noise effects on self-interference cancellation in full-duplex ofdm radio transceivers. *Wireless Communications, IEEE Transactions on*, 13(6):2977–2990, June 2014.

[59] E. Ahmed, A.M. Eltawil, and A. Sabharwal. Self-interference cancellation with phase noise induced ici suppression for full-duplex systems. In *Global Communications Conference (GLOBECOM), 2013 IEEE*, pages 3384–3388, Dec 2013.

[60] D.W. Bliss, T.M. Hancock, and P. Schniter. Hardware phenomenological effects on cochannel full-duplex mimo relay performance. In *Signals, Systems and Computers (ASILOMAR), 2012 Conference Record of the Forty Sixth Asilomar Conference on*, pages 34–39, Nov 2012.

[61] E. Ahmed, A.M. Eltawil, and A. Sabharwal. Self-interference cancellation with nonlinear distortion suppression for full-duplex systems. In *Signals, Systems and Computers, 2013 Asilomar Conference on*, pages 1199–1203, Nov 2013.

[62] M.A. Khojastepour and S. Rangarajan. Wideband digital cancellation for full-duplex communications. In *Signals, Systems and Computers (ASILOMAR), 2012 Conference Record of the Forty Sixth Asilomar Conference on*, pages 1300–1304, Nov 2012.

[63] Na Li, Weihong Zhu, and Haihua Han. Digital interference cancellation in single channel, full duplex wireless communication. In *Wireless Communications, Networking and Mobile Computing (WiCOM), 2012 8th International Conference on*, pages 1–4, Sept 2012.

[64] Junghwan Kim, K. Shamaileh, S. Adusumilli, and V. Rao. Digital interference cancellation for multimedia transmission in full duplex communication link. In *Broadband Multimedia Systems and Broadcasting (BMSB), 2013 IEEE International Symposium on*, pages 1–5, June 2013.

[65] D. Korpi, T. Riihonen, V. Syrjala, L. Anttila, M. Valkama, and R. Wichman. Full-duplex transceiver system calculations: Analysis of adc and linearity challenges. *Wireless Communications, IEEE Transactions on*, 13(7):3821–3836, July 2014.

[66] Yingbo Hua, Ping Liang, Yiming Ma, A.C. Cirik, and Qian Gao. A method for broadband full-duplex mimo radio. *Signal Processing Letters, IEEE*, 19(12):793–796, Dec 2012.

[67] D. Korpi, L. Anttila, V. Syrjala, and M. Valkama. Widely linear digital self-interference cancellation in direct-conversion full-duplex transceiver. *Selected Areas in Communications, IEEE Journal on*, 32(9):1674–1687, Sept 2014.

[68] V. Syrjala and K. Yamamoto. Sampling jitter in full-duplex radio transceivers: Estimation and mitigation. In *Acoustics, Speech and Signal Processing (ICASSP), 2014 IEEE International Conference on*, pages 2764–2768, May 2014.

[69] Qualcomm. www.qualcomm.com/invention/technologies/lte/lte-carrier-aggregation.

[70] LTE U Forum. www.lteuforum.org.

[71] Qualcomm. www.qualcomm.com/invention/technologies/lte/unlicensed.

[72] S. Katti Bharadia, K. R. Joshi. Robust full duplex radio link. pages 147–148. ACM, 2014.

[73] Yang-Seok Choi and H. Shirani-Mehr. Simultaneous transmission and reception: Algorithm, design and system level performance. *Wireless Communications, IEEE Transactions on*, 12(12):5992–6010, December 2013.

[74] Zhaowu Zhan, G. Villemaud, and J.-M. Gorce. Design and evaluation of a wideband full-duplex ofdm system based on aasic. In *Personal Indoor and Mobile Radio Communications (PIMRC), 2013 IEEE 24th International Symposium on*, pages 68–72, Sept 2013.

[75] M. Duarte, A. Sabharwal, V. Aggarwal, R. Jana, K.K. Ramakrishnan, C.W. Rice, and N.K. Shankaranarayanan. Design and characterization of a full-duplex multiantenna system for wifi networks. *Vehicular Technology, IEEE Transactions on*, 63(3):1160–1177, March 2014.

[76] K. Haneda, E. Kahra, S. Wyne, C. Icheln, and P. Vainikainen. Measurement of loop-back interference channels for outdoor-to-indoor full-duplex radio relays. In *Antennas and Propagation (EuCAP), 2010 Proceedings of the Fourth European Conference on*, pages 1–5, April 2010.

[77] Wei Zhou, G. Villemaud, and T. Risset. Full duplex prototype of ofdm on gnuradio and usrps. In *Radio and Wireless Symposium (RWS), 2014 IEEE*, pages 217–219, Jan 2014.

[78] S. Rajagopal, R. Taori, and S. Abu-Surra. Self-interference mitigation for in-band mmwave wireless backhaul. In *Consumer Communications and Networking Conference (CCNC), 2014 IEEE 11th*, pages 551–556, Jan 2014.

[79] A. Sahai, G. Patel, and A. Sabharwal. Asynchronous full-duplex wireless. In *Communication Systems and Networks (COMSNETS), 2012 Fourth International Conference on*, pages 1–9, Jan 2012.

[80] D.W. Bliss, P.A. Parker, and A.R. Margetts. Simultaneous transmission and reception for improved wireless network performance. In *Statistical Signal Processing, 2007. SSP '07. IEEE/SP 14th Workshop on*, pages 478–482, Aug 2007.

[81] D. Senaratne and C. Tellambura. Beamforming for space division duplexing. In *Communications (ICC), 2011 IEEE International Conference on*, pages 1–5, June 2011.

[82] Byungjin Chun and Hyuncheol Park. A spatial-domain joint-nulling method of self-interference in full-duplex relays. *Communications Letters, IEEE*, 16(4):436–438, April 2012.

[83] Y. Hua. An overview of beamforming and power allocation for mimo relays. In *MILITARY COMMUNICATIONS CONFERENCE, 2010 - MILCOM 2010*, pages 375–380, Oct 2010.

[84] D.W. Bliss and Y. Rong. Effects of channel estimation errors on in-band full-duplex mimo radios using adaptive transmit spatial mitigation. In *Signals, Systems and Computers, 2013 Asilomar Conference on*, pages 9–13, Nov 2013.

[85] Shenghong Li and R.D. Murch. An investigation into baseband techniques for single-channel full-duplex wireless communication systems. *Wireless Communications, IEEE Transactions on*, 13(9):4794–4806, Sept 2014.

[86] D. Korpi, S. Venkatasubramanian, T. Riihonen, L. Anttila, S. Otewa, C. Icheln, K. Haneda, S. Tretyakov, M. Valkama, and R. Wichman. Advanced self-interference cancellation and multiantenna techniques for full-duplex radios. In *Signals, Systems and Computers, 2013 Asilomar Conference on*, pages 3–8, Nov 2013.

[87] Pawinee Meerasri, Peerapong Uthansakul, and Monthippa Uthansakul. Self-interference cancellation-based mutual-coupling model for full-duplex single-channel mimo systems. *International Journal of Antennas and Propagation*, 2014, 2014.

[88] T. Riihonen and R. Wichman. Analog and digital self-interference cancellation in full-duplex mimo-ofdm transceivers with limited resolution in a/d conversion. In *Signals, Systems and Computers (ASILOMAR), 2012 Conference Record of the Forty Sixth Asilomar Conference on*, pages 45–49, Nov 2012.

[89] Zhaowu Zhan, G. Villemaud, and J.-M. Gorce. Analysis and reduction of the impact of thermal noise on the full-duplex ofdm radio. In *Radio and Wireless Symposium (RWS), 2014 IEEE*, pages 220–222, Jan 2014.

[90] T. Riihonen, S. Werner, and R. Wichman. Optimized gain control for single-frequency relaying with loop interference. *Wireless Communications, IEEE Transactions on*, 8(6):2801–2806, June 2009.

[91] T. Riihonen, A. Balakrishnan, K. Haneda, S. Wyne, S. Werner, and R. Wichman. Optimal eigenbeamforming for suppressing self-interference in full-duplex mimo relays. In *Information Sciences and Systems (CISS), 2011 45th Annual Conference on*, pages 1–6, March 2011.

[92] E. Antonio-Rodriguez, R. Lopez-Valcarce, T. Riihonen, S. Werner, and R. Wichman. Adaptive self-interference cancellation in wideband full-duplex decode-and-forward mimo relays. In *Signal Processing Advances in Wireless Communications (SPAWC), 2013 IEEE 14th Workshop on*, pages 370–374, June 2013.

[93] Bei Yin, M. Wu, C. Studer, J.R. Cavallaro, and J. Lilleberg. Full-duplex in large-scale wireless systems. In *Signals, Systems and Computers, 2013 Asilomar Conference on*, pages 1623–1627, Nov 2013.

[94] T. Riihonen, M. Vehkapera, and R. Wichman. Large-system analysis of rate regions in bidirectional full-duplex mimo link: Suppression versus cancellation. In *Information Sciences and Systems (CISS), 2013 47th Annual Conference on*, pages 1–6, March 2013.

[95] M. Vehkapera, T. Riihonen, and R. Wichman. Asymptotic analysis of full-duplex bidirectional mimo link with transmitter noise. In *Personal Indoor and Mobile Radio Communications (PIMRC), 2013 IEEE 24th International Symposium on*, pages 1265–1270, Sept 2013.

[96] P. Larsson and M. Prytz. Mimo on-frequency repeater with self-interference cancellation and mitigation. In *Vehicular Technology Conference, 2009. VTC Spring 2009. IEEE 69th*, pages 1–5, April 2009.

[97] D. Choi and D. Park. Effective self interference cancellation in full duplex relay systems. *Electronics Letters*, 48(2):129–130, January 2012.

[98] Cheulsoon Kim, Eui-Rim Jeong, Youngchul Sung, and Y.H. Lee. Asymmetric complex signaling for full-duplex decode-and-forward relay channels. In *ICT Convergence (ICTC), 2012 International Conference on*, pages 28–29, Oct 2012.

[99] E. Antonio-Rodriguez, R. Lopez-Valcarce, T. Riihonen, S. Werner, and R. Wichman. Autocorrelation-based adaptation rule for feedback equalization in wideband full-duplex amplify-and-forward mimo relays. In *Acoustics, Speech and Signal Processing (ICASSP), 2013 IEEE International Conference on*, pages 4968–4972, May 2013.

[100] R. Lopez-Valcarce, E. Antonio-Rodriguez, C. Mosquera, and F. Perez-Gonzalez. An adaptive feedback canceller for full-duplex relays based on spectrum shaping. *Selected Areas in Communications, IEEE Journal on*, 30(8):1566–1577, September 2012.

[101] E. Antonio-Rodriguez and R. Lopez-Valcarce. Adaptive self-interference suppression for full-duplex relays with multiple receive antennas. In *Signal Processing Advances in Wireless Communications (SPAWC), 2012 IEEE 13th International Workshop on*, pages 454–458, June 2012.

[102] E. Antonio-Rodriguez and R. Lopez-Valcarce. Cancelling self-interference in full-duplex relays without angle-of-arrival information. In *Acoustics, Speech and Signal Processing (ICASSP), 2013 IEEE International Conference on*, pages 4731–4735, May 2013.

[103] K. Hayashi, Y. Fujishima, M. Kaneko, H. Sakai, R. Kudo, and T. Murakami. Self-interference canceller for full-duplex radio relay station using virtual coupling wave paths. In *Signal Information Processing Association Annual Summit and Conference (APSIPA ASC), 2012 Asia-Pacific*, pages 1–5, Dec 2012.

[104] K. Hayashi, M. Kaneko, M. Noguchi, and H. Sakai. A single frequency full-duplex radio relay station for frequency domain equalization systems. In *Communications in China (ICCC), 2013 IEEE/CIC International Conference on*, pages 33–38, Aug 2013.

[105] M. Nagahara, H. Sasahara, K. Hayashi, and Y. Yamamoto. Sampled-data h ; design of couplingwave cancelers in single-frequency full-duplex relay stations. In *SICE Annual Conference (SICE), 2014 Proceedings of the*, pages 401–406, Sept 2014.

[106] S.O. Al-Jazzar and T. Al-Naffouri. Relay self interference minimisation using tapped filter. In *Systems, Signal Processing and their Applications (WoSSPA), 2013 8th International Workshop on*, pages 316–319, May 2013.

[107] E. Everett, D. Dash, C. Dick, and A. Sabharwal. Self-interference cancellation in multi-hop full-duplex networks via structured signaling. In *Communication, Control, and Computing (Allerton), 2011 49th Annual Allerton Conference on*, pages 1619–1626, Sept 2011.

[108] A. Thangaraj, R.K. Ganti, and S. Bhashyam. Self-interference cancellation models for full-duplex wireless communications. In *Signal Processing and Communications (SPCOM), 2012 International Conference on*, pages 1–5, July 2012.

[109] P. Meerasri, P. Uthansakul, and M. Uthansakul. Performance of self and mutual interference cancellation for fdsc mimo systems. In *Electrical Engineering/Electronics, Computer, Telecommunications and Information Technology (ECTI-CON), 2014 11th International Conference on*, pages 1–5, May 2014.

[110] Jun Wang, Hongzhi Zhao, and Youxi Tang. A rf adaptive least mean square algorithm for self-interference cancellation in co-frequency co-time full duplex systems. In *Communications (ICC), 2014 IEEE International Conference on*, pages 5622–5627, June 2014.

[111] Jong-Ho Lee and Yong-Hwa Kim. Compressed channel sensing using designated null subcarriers in full duplex wireless ofdm systems. *Wireless Personal Communications*, 79(3):1635–1645, 2014.

[112] Andreas Polydoros, Michael Fitz, Scott Enserink, Gautam Thatte, and Thomas Halford. Tethered interference cancellation: Military versus full-duplex applications and comparisons. In *European Wireless 2014; 20th European Wireless Conference; Proceedings of*, pages 1–5, May 2014.

[113] Zhaojun He, Shihai Shao, Ying Shen, Chaojin Qing, and Youxi Tang. Performance analysis of rf self-interference cancellation in full-duplex wireless communications. *Wireless Communications Letters, IEEE*, 3(4):405–408, Aug 2014.

[114] N. Verhoeckx, H. van den Elzen, F. Snijders, and P. van Gerwen. Digital echo cancellation for baseband data transmission. *Acoustics, Speech and Signal Processing, IEEE Transactions on*, 27(6):768–781, Dec 1979.